https://doi.org/10.5194/tc-2021-363
Preprint. Discussion started: 23 December 2021

The Cryosphere Discussions

Synoptic control over winter snowfall variability observed in a remote site of Apennine Mountains (Italy), 1884-2015

Vincenzo Capozzi, Carmela De Vivo, Giorgio Budillon

Department of Science and Technology, University of Naples "Parthenope", Centro Direzionale di Napoli – Isola C4, 80143, Naples, Italy

Correspondence to: Vincenzo Capozzi (vincenzo.capozzi@collaboratore.uniparthenope.it)

Abstract. This work presents a new, very long snowfall time series collected in a remote site of Italian Apennine mountains (Montevergine Observatory, 1280 m a.s.l.). After a careful check, based on quality control tests and homogenization procedures, the available data (i.e. daily height of new snow) have been aggregated over winter season (December-January-February) to study the long-term variability in the period 1884-2020. The main evidences emerged from this analysis lie in (i) the strong interannual variability of winter snowfall amounts, in (ii) the absence of a relevant trend from late 19th century to mid-1970s, in (iii) the strong reduction of the snowfall amount and frequency of occurrence from mid-1970s to the end of 1990s (-45 and -17% compared to the average recorded in 1884-1975 period, respectively), and in (iv) the increase of average snowfall amount and frequency of occurrence in the last 20 years.

Moreover, this study shed light on the relationship between the snowfall variability observed in Montevergine and the large-scale atmospheric circulation. Six different synoptic types, describing the meteorological scenarios triggering the snow events in the study area, have been identified by means of a cluster analysis, using two essential atmospheric variables, the 500-hPa geopotential height and the sea level pressure (both retrieved from the third version of Twentieth Century Reanalysis dataset). Such patterns trace out scenarios characterized by the presence of a blocking high-pressure anomaly over Scandinavia or North Atlantic and by a cold air outbreak, involving both maritime and continental cold air masses. A further analysis demonstrates that the identified synoptic types are strongly related with different teleconnection patterns, i.e. the Arctic Oscillation (AO), the Eastern Atlantic Western Russia (EAWR), the Eastern Mediterranean Pattern (EMP), the North Atlantic Oscillation (NAO) and the Scandinavia pattern (SCAND), that govern the European winter atmospheric variability. The relevant decline in snowfall frequency and amounts between 1970s and 1990s can be mainly ascribed to the strong positive trend of AO and NAO indices, which determined, in turn, a decrease in the incidence of patterns associated to the advection, in central Mediterranean area, of moist and cold arctic maritime air masses. The recent increase in average snowfall amounts can be explained by the reverse trend of AO index and by the prevalence of neutral or negative EAWR pattern.

1 Introduction

In recent years, the studies focused on past and present snowfall variability have gained more and more attention within the scientific community. It is widely recognized, in fact, that snow exerts a relevant impact within the hydrological cycle,

https://doi.org/10.5194/tc-2021-363
Preprint. Discussion started: 23 December 2021

providing a fundamental reservoir of fresh water, as well as in the whole climate system, controlling the land surface albedo in the global energy budget (e.g. Armstrong and Brun, 2008; Wilson et al., 2010). As well explained by Irannezhad et al. (2017), the occurrence of snowfall events is the results of a delicate balance between thermal and hygrometric conditions and, therefore, it is extremely susceptible to processes and feedback mechanism triggered by global climate change (Berghuijs et al., 2014).

Several studies reported interesting evidences about last 10-years periods snowfall variability. As an example, less frequent but more severe snowstorms have been observed in the USA (Chagnon, 2007). In the Pyrenees region (Spain), Lopez-Moreno et al. (2011) have found an altitude-dependent behaviour of snowfall intensity. After mid-1970s, a relevant decrease in the number of snowfall days has been detected by Pons et al. (2010) in the northern part of the Iberian Peninsula; according to the authors findings, such evidence is the result of an increase in temperature at low elevations and of a decrease in the precipitation recorded at high altitudes. A further focus on the Iberian Peninsula, and in particular on Castilla y Leon region, was provided by Merino et al. (2014), which highlighted a negative trend in snowfall days for the period 1960-2011, as well as interesting linkages between regional snowfall variability and large-scale atmospheric patterns. Recently, Marcolini et al. (2017) investigated the snow depth time series collected in the Adige basin (North East Italy) for the period 1980-2019. According to the results of this study, a relevant reduction of both snow cover duration and mean seasonal snow depth occurred in the Adige catchment after 1988, both at low and high elevation sites. On the contrary, in the period from 2000 to 2009, an increase (although not identified as statistically significant) of mean seasonal snow depth has been recorded. A very comprehensive assessment of snow depth trends in the European Alps has been presented by Matiu et al. (2021). The latter observed negative trends in snow cover in the period from 1971 to 2019, especially in spring season. Moreover, this study highlights that mean snow depth in the Alpine region has a very strong interannual variability and that it exhibited a very strong decline in the 1990s, followed by a partial recovery from 2000s.

The study period of the climatological researches carried out in such works is generally limited to the last 55-65 years. However, few studies stretched further back their analysis, due to the absence, in many areas, of reliable and continuous old snowfall climatological records. In this respect, an important reference for mountainous area is Laternser and Schreebel (2003), who discovered, for the Swiss Alps, an increase in snow cover and duration from 1930 to early 1980 and, subsequently, a statistically significant decrease towards 1999. Some years later, Hartmett et al. (2014) reported a significant increase in observed snowfall in Central New York State (USA) during the last 80 years (1931-2012). More recently, Irannezhad et al. (2017) evaluated the annual snowfall variability in Finland in 1909-2008 period, analysing its relationship with some large-scale atmospheric patterns.

This study aims providing a new contribution to this research path, by analysing the snowfall variability observed in the last 137 years (1884-2020) in a remote site of Southern Apennine Mountains, Montevergine observatory (40.936502° N, 14.729150° E), located in Campania region at 1280 m above sea level (a.s.l.).

As well highlighted in some previous studies (Diodato, 1992; Capozzi and Budillon, 2017; Capozzi et al., 2020), Montevergine climatic series has some distinguishing features, mainly related to its longevity (it is the oldest collected in the Apennine region

https://doi.org/10.5194/tc-2021-363
Preprint. Discussion started: 23 December 2021

above 1000 a.s.l.) and to the environment in which it has been collected, i.e. a remote mountainous area of Central Mediterranean region. It is widely recognized that the impact of climate change on water resources and ecosystems is amplified in regions, such mountainous ones, were snowfall plays a relevant in role in precipitation regime (e.g. Irannezhad et al., 2017). In this respect, Montevergine's climatic records offer a relevant opportunity to extend, from both quantitative and qualitative perspectives, the current knowledge about the past snowfall variability observed in Mediterranean mountainous sectors. Moreover, we focused on the links between large-scale atmospheric patterns and local variability, which is a topic addressed by many papers (e.g. Sheridan and Lee, 2010; Cohen et al., 2013). More specifically, we have extracted six different synoptic patters that triggered the snow events occurred in Montevergine in winter season (defined as December-January-February) and we have studied the temporal behaviour of their occurrence frequency, as well as their links with some teleconnection indices that control the thermo-pluviometric regime in the Mediterranean region.

This paper has been structured as follows. Section 2 presented Montevergine snowfall time series, describing the procedures adopted for quality control and homogenization; moreover, it provides details about data and methodologies used to establish the synoptic scale patterns, as well as a brief description of the teleconnection indices involved in this study. The results are sketched in section 3, whereas section 4 is dedicated to the relationships between the identified synoptic types and teleconnections. Finally, the concluding remarks are provided in Section 5.

2 Materials and methods

2.1 Study area, data source and measurements practices

The snowfall climatological time series involved in this study has been collected in Montevergine Observatory (hereafter, MVOBS). The latter is located in Campania Region (Southern Italy) on the eastern side of the Partenio Mountains, which are part of the Southern Apennines (Fig. 1, left panel). As clearly highlighted in some previous papers (e.g. Capozzi et al., 2017; Capozzi et al., 2020), MVOBS has a very complex meteorological regime, modulated by a large spectrum of synoptic patterns. Its geographical position, in fact, barycentric with respect to the Mediterranean Sea and Balkan regions, results in the frequent incidence of moist air masses coming from near Atlantic and Mediterranean basins as well as of cold outbreaks coming from Northern and Eastern Europe. Both weather types are associated to precipitation events, which are sometimes empathized by local orographic features. Considering the last climatological reference period (1981-2010), MVOBS receives an average annual precipitation of 1606.8 mm (± 338.0 mm), with maxima average amounts in winter (527.8 ± 191 mm) and fall (518.5 ± 186 mm) seasons, and a minimum in summer (163.0 ± 88 mm). It is important pointing out that if we consider the entire observational period, which spans from 1884 up to date, the annual average precipitation rises to around 2100 mm. As it will be discussed in section 3, a strong and relevant reduction of precipitation amounts has been recorded between mid-1970s and late 1990s.

The meteorological observation in MVOBS started on January 1, 1884, under the management of the "Italian Central Office of Meteorology and Geodynamics" (hereafter, the Italian Central Office, ICO), which was established in Rome in 1879

https://doi.org/10.5194/tc-2021-363
Preprint. Discussion started: 23 December 2021

(Maugeri et al., 1998). Since from first years, the observatory was equipped with many instruments, most of them placed on a meteorological tower, built up on the eastern side of the Montevergine Abbey in 1895 (Capozzi et al., 2020). According to the available metadata, the nivometric measurements started on 01 April 1884; in compliance with the recommendations of the ICO, the snowfall measures have been performed manually using a traditional nivometer. The latter consists of a snowboard and of a graduated yardstick with an area of 0.01 m^2 and a section of 0.0001 m^2, respectively. The snow observations consist of two essential variables, the height of new snow (i.e. the amount of fresh snow with respect to the previous observations, hereafter HNS) and the snow depth (i.e. the vertical distance from the snow surface to the soil level, hereafter SD). The measurements have been collected in the "*Giardinetto dell'Ave Maria*", a cloister located next to the northern side of the meteorological tower (Fig. 1, right panel).

The standards in terms of measurement instrument and location have not changed over the course of time. The measurements practices frequently changed over time, depending by the standards prescribed by the reference government or military offices, instead. Detailed and useful information about the specific period covered by each parameter involved in nivometric measurements are presented in Fig. 2 (left panel). More specifically, in some time intervals both daily (hereafter, HNSd and SDd) and sub-daily data (hereafter, HNSsd and SDsd) are available. The left panel of Fig. 2 shows that near-continuous observations (data availability = 95.7% for the 1884-2020 period) are available only for HNSd (blue line), which presents a relevant gap in 1964-1968 period when MVOBS was suspended due to lack of personnel. The HNSsd observations (red line) were carried out only between 1892 and 1963; more specifically, from 1892 to 1932 sub-daily records were collected at 09:00, 15:00 and 21:00 local time, whereas from 1933 to 1963 the three daily data were acquired at 08:00, 14:00 and 19:00 local time. Regarding the SD, this variable was sporadically collected in the periods November 1944 – March 1952 and November 1953 – May 1961 and then more continuously (although only on a daily basis) from 1969 to 2008 (black line).

The snowfall data, as well as the other meteorological records, were stored in paper-based registers, containing the daily and sub-daily observations collected for each year (Capozzi et al., 2020). Figure 2 (right panel) shows an extract of the meteorological register for the data measured in the second decade of January 1946. The register is formatted in tables according to the standards suggested by the ICO. The columns storing the SDsd (22-24, starting from the left), HNSsd (25-27) and the HNSd (28) data are bordered in red for the convenience of the reader. All values are expressed in centimetres (cm).

The entire dataset has been transcribed into a digital support by the Department of Science and Technology of the University of Naples "Parthenope", using a simple "key entry" approach (Brönnimann et al., 2006). A part of the dataset, including the sub-daily meteorological data collected between 1884 and 1963, is publicly available from the National Oceanic and Atmospheric Administration (NOAA) - National Centers for Environmental Information (NCEI) repository (Capozzi et al., 2019).

It is worth of mention that manual snowfall measurements have several limitations, which are well summarized and discussed in WMO (2008). Such uncertainties rely in observer's errors in reading and recording the measure and in poor siting. The use, as in the context of Montevergine, of a single stake could result in large errors, depending on the site mean variability: according to WMO (2008), this error increase with decreasing of snow depth. The limitations related to the siting area may be

https://doi.org/10.5194/tc-2021-363
Preprint. Discussion started: 23 December 2021

exacerbated by environmental conditions, such as strong winds and/or turbulence, which may generate snow drifts and spatial inhomogeneity in snow depth. According to verbally transmitted information (provided to the authors of this paper by the Benedictine Community of Montevergine), to mitigate the occurrence of poor siting conditions (mainly caused by strong winds), the snow depth value taken from reference observation (collected with a fixed stake) was replaced by an average snow depth value coming from spatially distributed non-fixed observations. Unfortunately, the use of this alternative measurements method has not been systematically mentioned in the meteorological registers or in metadata.

2.2 Quality control and homogenization

It is well known that the consistency and the reliability of an historical climatological time series can be undermined by several errors and artefacts, dealing with human mistakes in data collection, inaccuracies in digitization procedures and instrument failures. For this reason, as highlighted by many papers (e.g. Ashcroft et al., 2018), it is essential applying a Quality Control (QC) procedure to identify both systematic and non-systematic errors.

However, in meteorological and climatological fields, there is not an unambiguous and universal QC strategy. Depending on the number of data, in fact, different methods can be employed. As an example, in a scenario involving a large dataset including high-resolution data, it is possible opting for methods that allow not only identifying anomalous values, but also to devise criteria for correcting them. On the other hand, for a single isolated time series, such as the one considered in this work, it is convenient select simpler methods that are able to accept or reject a determined observation depending on statistical objective criteria.

In this study, following the guidelines provided by WMO (2011) and by the Istituto Superiore per la Protezione e la Ricerca Ambientale (ISPRA), we developed a QC strategy based on two different statistical test, the gap check and the climatological control (ISPRA, 2016). Both tests are designed to detect the outliers, i.e. the anomalous data that exceed specific limits defined according to an objective probability distribution model or to specific climatological values.

More specifically, the gap check detects unrealistic breaks in the frequency distribution of a temperature or precipitation data sample. We have applied this method as follows. Firstly, for each month we have sorted in ascend order the HNSd data recorded over the entire available period (1884-2020). Subsequently, we have calculated the difference between two-consecutive values: if a certain HNSd value is at least 35 cm larger than the previous record, then that value and subsequent ones are flagged as outliers. In the selection of the just mentioned threshold (35 cm), we followed the guidelines and the suggestions provided by NCEI of NOAA (Durre et al., 2010). As testified by Fig. 3, which shows the frequency distribution of HNSd for winter months (December, January and February), no outliers were detected by gap check.

The second procedure, the climatological control, checks for HNSd values that go beyond the respective 29-days climatological 95th percentiles by at least a certain factor (which is equal to 5 according to the recommendations of NOAA's NCEI). We

https://doi.org/10.5194/tc-2021-363
Preprint. Discussion started: 23 December 2021

have applied this method to each calendar day, considering the entire available time series (1884-2020). The results confirm the very encouraging findings of gap check: no outliers, in fact, have been detected.

In addition to quality control, it is common practice to apply statistical methods to climatological observations in order to verify the time series homogeneity and identify the possible presence of artificial shifts or trends that can affect the results of data analysis (Wijngaard et al., 2003; Hänsel et al., 2016). More specifically, the inhomogeneity in climatic data can be attributed to several factors, including instrumentation error, changes in the environment adjacent to the instrument and human mishandling.

We applied two methods to detect and locate abrupt changes in the snowfall time series involved in this study, namely the Pettitt test (Pettitt, 1979) and CUSUM test (Smadi et Zghoul, 2006; Hänsel et al., 2016; Patakamuri et al., 2020; Gadedjisso-Tossou et al., 2021).

The Pettitt test for change detection, developed by Pettitt (1979), is a non-parametric rank test, which is useful for evaluating the occurrence of abrupt changes in climatic records (Sneyers, 1990; Smadi and Zghoul 2006; Verstraeten et al., 2006; Mu et al., 2007; Zhang and Lu, 2009; Gao et al., 2011). It is the most commonly used test for change point detection because of its sensitivity to breaks in the middle of any time series (e.g. Winingaard et al., 2003).

The ranks $r_1 \ldots r_n$ of a determined time series $Y_{i=1 \ldots n}$ are used to calculate the statistics test X as:

$$X_k = 2 \sum_{i=1}^{k} r_i - k(n+1) \quad (1)$$

where $k = 1, 2 \ldots n$ is a determined observation of the series.

When a break occurs at year K, the statistic is maximum or minimum at year $k = K$,

$$X_K = \max_{1 \le k \le n} |X_k| \quad (2)$$

The value of X_K is compared with a critical value given by Pettitt (1979) to test for statistical significance (Patakamuri et al. 2020).

On the other hand, the CUSUM approach is based on the analysis of the chronological series of the cumulative sums of deviations between a determined observation and the sample mean.

For a determined series $Y_{i=1..n}$, the CUSUM value (CS_i) at any time i is given as:

$$CS_i = (Y_i + Y_{i-1} + Y_{i-2} \ldots . + Y_n) - i \ldots . \bar{x} \quad (3)$$

where n is sample size and $\bar{x}$ the average of the total series.

https://doi.org/10.5194/tc-2021-363
Preprint. Discussion started: 23 December 2021

When the series under test is free from any inhomogeneity, the plot of CS_i versus i should normally oscillate around the horizontal axis. A steady decline or rise of this plot (or drastic departure from oscillatory patterns in that regard) would suggest the possibility of an artificial break point from the year of observation (corresponding to the year i) of such a change.

These tests are generally performed under two hypotheses: H0 (null hypothesis), i.e. data are homogeneous; and Ha (alternative hypothesis), i.e. there is a date on which a change in the series occurs. When a p-value is lower than the significance level, generally 5%, H0 hypothesis should be rejected and Ha hypothesis accepted (Gadedjisso-Tossou et al., 2021).

The two homogeneity tests were performed using the "Anabasi 2018 version 1.51 beta" (ANAlisi statistica di BAse delle Serie storiche di dati Idrologici), a specific tool developed by ISPRA in the Visual Basic for Application language (Braca et al., 2013).

We applied both tests to the monthly HNS climatological series. The results obtained from the application of Pettitt and CUSUM tests through the Anabasi tool did not reveal any change points in the historical series.

2.3 Reanalysis data

The reanalysis data represent a very commonly used product in studies concerning the examination of atmospheric circulation patterns and their correlation with local climate variability (e.g. King and Turner, 1997; Cohen et al., 2013).

In this work, we used the Twentieth Century Reanalysis dataset (20CR), which has been generated by the NOAA and by the University of Colorado Boulder's Cooperative Institute for Research in Environmental Sciences (CIRES), in partnership with the International Atmospheric Circulation Reconstructions over the Earth Initiative (ACRE; Atlas et al., 2011). More specifically, we selected the latest version of this dataset (the version 3), which has been launched by NOAA, CRIES and the U.S. Department of Energy (DOE). The NOAA-CIRES-DOE 20CR Version 3 (20CRV3) provides a four-dimensional global atmospheric dataset spanning from 1836 to 2015 at 1.0° latitude/longitude resolution. Main advances of this product with respect to the previous versions lie in the improved data assimilation system, in the assimilation of a large set of observations and in the usage of newer and higher resolution models (Slivinski et al., 2019).

To characterize the synoptic conditions that triggered the snow events in the site of interest, we focused on two parameters: the 500-hPa geopotential height (hereafter, Z500) and the sea-level atmospheric pressure (hereafter, SLP). The first one can be considered a "primary" meteorological field, giving essential information about large-scale mid-tropospheric flow as well as about the location and intensity of ridges, troughs and sub-synoptical patterns (i.e. upper level lows). The SLP is a "secondary" atmospheric field, providing information about location and intensity of main surface synoptic features, such as low and high-pressure systems, which can be regarded as the result of dynamical and thermodynamical processed that involve the entire tropospheric column.

For the purposes of this work, we extracted from 20CRV3 the daily (00:00 UTC) Z500 and SLP data for the winter seasons (01 December-28 February) of the 1884-2015 time period, considering an area that includes the entire European territory (25-

https://doi.org/10.5194/tc-2021-363
Preprint. Discussion started: 23 December 2021

90°N, -45°W-65°E). This region appears to be reasonably representative of the synoptic conditions that control the meteorological regime of the site of interest.

2.4 Cluster analysis

Among the different methodologies and approaches usually involved in synoptic types classification, we have selected the cluster analysis (CA). The latter is an unsupervised learning technique that aims finding natural grouping and pattern in a determined data set. The literature offers several example of application of CA (e.g. Kidson, 1994a; Kidson, 1994b; Kidson, 2000; Cohen et al., 2013), involving some essential synoptic variables, such as the mean sea level pressure field and the 1000, 700 and 500-hPa geopotential heights.

In this study, we have applied the CA as follows. Firstly, using the available 20CRV3 reanalysis data, we have computed the Z500 and SLP anomalies, considering the 1981-2010 as climatological mean reference. Subsequently, we have selected the wintertime days in which snowfall precipitation has been observed in MVOBS. In this respect, for CA we have considered as "snowy" a day in which the recorded HNSd value was at least 3 cm. This threshold allows filtering out most of some ambiguous events, characterized by the simultaneous presence of different hydrometeors types (i.e. rain, snow hail or graupel). Using this criterion, the time-dimension of the dataset, originally including 50039 time points (i.e. all winter days between 1884 and 2015), reduces to 1986 days. Prior to clustering, the selected data were subjected to a Principal Component Analysis (PCA). This approach is commonly adopted (e.g. Yeung and Ruzzo, 2001) in order to reduce the dimensionality of the data set and, consequently, the computational cost of CA. For both parameters (Z500 and SLP), we have considered the first eight PCA components; the latter, according to the scree plots (Fig. 4), explain over the 80% of the total variance (more specifically, the 83.8% for Z500 and the 89.0% for SLP). After this pre-processing, we have applied the well-known k-means method (MacQueen, 1967) using as input the 16 components resulting from PCA. Following standard procedures to assess cluster reproducibility and stability, we have performed several sensitivity experiments, by running the k-mean procedures using different randomly selected seed clusters. The final selection of the optimal number of clusters has been performed by manual inspection. According to this strategy, six different clusters were extracted: for each of them, we determined the frequency of occurrence for every winter season, as well as other basic statistical indicators, such as the associated average and standard deviation of HNSd values.

The synoptic type classification is a powerful and descriptive tool for summarizing the typical modes of atmospheric circulation that affects local climatic features. However, it should bear in mind that the identification of discrete categories presents several limits, mainly related to (i) the challenges in identify the boundaries between synoptic classes (i.e. patterns may switch abruptly, but in some occasion there is gradual transition from a pattern to another one), (ii) the impact of minor features, such as weak low or transitory ridge, that may not negligible in some circumstances and (iii) to the seasonal variation in type characteristics (i.e. synoptic features are generally most relevant in winter).

https://doi.org/10.5194/tc-2021-363
Preprint. Discussion started: 23 December 2021

2.5 Teleconnections

To investigate the relationships between large-scale climate variability and the synoptic types identified in this study, we have considered five different teleconnections: the Arctic Oscillation (AO), the East Atlantic Western Russia (EAWR), the Eastern Mediterranean Pattern (EMP), the North Atlantic Oscillation (NAO) and the Scandinavian Pattern (SCAND). These large-scale modes are known to have relevant influences on the atmospheric circulation of Mediterranean area, especially in winter season. For the convenience of the reader, we provide below a brief description of each teleconnection:

- AO: it is one of the leading mode of the northern hemisphere climate variability, describing the circulation pattern over the mid-to-high latitudes. The positive phase of this mode is associated to a ring of strong winds circulation around North Pole and is synonymous of a vigorous polar vortex, confining the cold air across northern latitudes. When negative phase occurs, the belt of winds became weaker and the polar front is subjected to relevant oscillations, resulting in cold air masses outbreaks across mid-latitudes.
- EAWR: it is a prominent teleconnection pattern that affects the Eurasia throughout year (Barnston and Livezey, 1987). It consists of four main Z500 anomaly centres, placed in sequence from west to east in the latitude range between 40 and 70°N. The EAWR positive phase is characterized by positive Z500 anomalies over Europe and northern China, and negative height anomalies over the central North Atlantic and north of the Caspian Sea. In the negative phase, the poles reverse and, therefore, Europe experiences negative Z500 anomalies.
- EMP: this pattern has been identified by Hatzaki et al. (2007) and it is defined as the difference in Z500 between the north-eastern Atlantic and the eastern Mediterranean. The positive phase is associated to a positive Z500 anomaly in the north Atlantic and to a negative Z500 anomaly across central and eastern Mediterranean area. This Z500 anomalies placement means, in winter season, favourable conditions to cold air outbreaks over central and southern Europe. Oppositely, the negative EMP phase means positive Z500 anomaly over the eastern Mediterranean and northern Africa, where predominates an anticyclonic circulation.
- NAO: it can be considered the Atlantic branch of the AO and it describes the sea-level pressure pattern between the Northern Atlantic Ocean (near Greenland and Iceland), where generally the air pressure is below than surrounding regions, and the Central Atlantic Ocean (near Portugal and Azores), which generally experiences air pressure higher than surrounding areas. The NAO positive phase means that both subpolar low and the subtropical high are stronger than average and that, consequently, the Atlantic jet stream is confined to high latitudes. The negative phase results in a weakening of both subpolar low and subtropical high and, therefore, in a southward shift of the storm track.
- SCAND: this pattern consists of a primary relevant circulation centre over Scandinavia and weaker poles of opposite sign over Western Europe and eastern Russia/western Mongolia. The positive phase, characterized by positive Z500 anomalies over Scandinavia region and western Russia, reflects synoptic scenarios that promote the formation of blocking anticyclones. During the opposite phase, negative Z500 anomalies prevail over Scandinavia area and weak positive anomalies over Western Europe.

https://doi.org/10.5194/tc-2021-363
Preprint. Discussion started: 23 December 2021

The AO, EAWR, EMP, NAO and SCAND indexes have been retrieved from the Climate Prediction Center (CPC) of the NOAA's National Weather Service, where monthly data from 1950 are available (https://www.cpc.ncep.noaa.gov/data/teledoc/telecontents.shtml). For each index, we have extracted the winter season time series by simply averaging, for a determined year, the monthly values of December (previous year), January and February. Regarding the EMP, its variability was ad-hoc reconstructed using the reanalysis data involved in this study (20CRV3 product), following the methodology suggested in Hatzaki et al. (2009). The EMP has been firstly reconstructed, for the 1950-2015 period, on a monthly basis; subsequently, the data have been standardized with respect to 1981–2010 climatology and averaged on winter season, in order to have a time series that is fully consistent with the ones available for the other teleconnection indices.

3 Results

3.1 Snowfall variability in 1884-2020 period

In this section, we present the evidences provided by the snowfall time series collected in MVOBS between 1884 and 2020. Figure 5 (left panel) presents the results in terms of total HNS observed in winter season year-by-year (blue bars). To filter out the high-frequency variability, we have applied a locally weighted scatter plot smooth (hereafter, lowess), highlighted as red curve, setting the time span equal to 10 years. The missing data are highlighted as yellow bars. A simple visual inspection of the signal allows identifying some relevant features: (i) the strong interannual variability, which is typical of precipitation records collected in mid-latitudes, and (ii) the strong reduction in snowfall amounts between mid-1970s and late 1990s. The latter evidence is in agreement with the findings of several previous studies (e.g. Laternser and Schreebel, 2003; Marcolini et al., 2017; Matiu et al. 2021). In order to examine the behaviour of winter HNS in MVOBS, we have subdivided the time series into six different sub-periods: 1884/85-1906/07, 1907/08-1929/30, 1930/31-1952/53, 1953/54-1974/75, 1975/76-1997/98 and 1998/99-2019/20. Table 1 shows, for each time segment, the average HNS value and the associated standard deviation. In the first period, almost all winter seasons were characterized by HNS total amounts greater than 100 cm, resulting in an average of 223.4 cm (the highest among all considered sub-periods). Subsequently (1907/08-1929/30), the average HNS value drops to 190.1 cm, due to a relevant but transitory reduction of snowfall amounts observed in the first part of 1920s. Among 1930s and 1950s, the average snowfall amounts rise to 205.4 cm, with a standard deviation (± 102.3 cm) similar to that observed in the previous segments. In the following sub- period (1953/54-1974/75), a further slight increase in average HNS amount has been detected. However, in this segment there is also a rise in standard deviation (± 152.3 cm), that can be explained by the occurrence of some seasons (1953/54 and 1955/56) characterized by excessive amounts (579 and 514 cm, respectively) as well as of meagre winters (1954/55, 1963/64 and 1974/75), in which the accumulated HNS was 16, 30 and 39 cm, respectively. It should be noted that the statistics of this period might be adversely affected by some missing data. In the second-to-last sub-period, there was an impressive reduction of snowfall accumulation (-45% with respect to the average of 1884-1975 period).

https://doi.org/10.5194/tc-2021-363
Preprint. Discussion started: 23 December 2021

The strong anomalies observed in this period are well emphasized not only by the average HNS value (which drops to 114.9 cm), but also by the standard deviation (which is ± 58.5 cm). According to Table 1, in the last time interval there was an increase in the average HNS amounts, although they are quite lower that those generally observed before 1970s.

Additional and relevant information about the variability of snowfall regime observed in MVOBS are provided by the right panel of Fig. 5, which shows the behaviour in time of the number of snowy days (NSD) occurred in winter between 1884/85 and 2019/20 seasons. In the first four sub-periods, the average NSD value fluctuates between 21 and 24 days and the standard deviation ranges from ± 8.4 to ± 9.9 days. Subsequently, in alignment with that observed for HNS, in the period from 1975/76 to 1997/98 there was a reduction in snowfall events frequency, which lowered to 18.2 days (± 7.5). The absolute minimum NSD value was observed in 1989/1990 season, when only 3 snowfall days occurred. The similarities with the evidences provided by the analysis of total winter HNS also rely in the reduction of NSD in the 1920s and in its slight recovery after 2000s. It is important to highlight that the NSD parameter presented in the right panel of Fig. 5 include days in which an HNS value of at least 1.0 cm has been recorded.

3.2 Synoptic types

In this section, we discuss the six synoptic types (ST) emerged from CA. Each pattern represents a typical synoptic scenario that is able triggering snowfall events in MVOBS. For the convenience of the reader, we labelled each cluster as follows: the first type, ST1, was named as “Arctic Maritime”, the second one, ST2, as “Central Europe Low”, the third one, ST3, as “Continental Air”, the fourth one, ST4, as “Mediterranean Low”, the fifth one, ST5, as “Arctic Trough” and the sixth one, ST6, as “Polar Maritime”.

Figure 6 shows the first three synoptic types, ST1, ST2 and ST3. More specifically, the left panels present, for each ST, the Z500 anomaly (in m), whereas the right panels the corresponding SLP anomalies (in hPa).

The ST1 (Arctic Maritime) shows a synoptic condition that promotes the incoming of cold arctic maritime air masses in central Mediterranean area. This pattern is typically the fruit of a relevant oscillation of polar front, triggered by a positive Z500 anomaly (Fig. 6a) over northern Atlantic, between Greenland and Iceland. In most of European territory, a trough elongated from northern to southern Europe conditions the atmospheric circulation. The latitudinal extension of negative Z500 anomaly suggests that this pattern represents, on average, the mature stage of the Rossby wave associated to the polar front oscillation, which results in strong thermal and pressure gradients. Because of this upper level circulation, the low-level conditions are modulated by two opposite poles (Fig. 6b), a positive SLP anomaly (up to 15 hPa) over northern Atlantic and a negative SLP anomaly over eastern Europe, Balkans and Central and Southern Italy. The scenario just described leads to the development of a strong baroclinicity in the area of interest, where very favourable conditions for snow events occur.

The ST2 (Fig. 6c,d) presents a synoptic situation modulated by a relevant negative Z500 anomaly over Central Europe (located, on average, between Eastern of France, Alpine region and Southwestern of Germany). This upper level anomaly can be

https://doi.org/10.5194/tc-2021-363
Preprint. Discussion started: 23 December 2021

considered the final stage of a Rossby wave that brings cold arctic maritime air masses from northern to central and southern Europe. This negative Z500 anomaly is counteracted by a positive anomaly over Greenland, north-western Atlantic and Arctic. This pattern results in a cyclonic circulation over Central Mediterranean area, well represented by a negative SLP anomaly on Central Italian peninsula, which triggers a cold and moist southwestern flow over the area of interest.

The ST3 (Continental Air) resembles a synoptic scenario that promotes the incoming in central Mediterranean basins of very cold continental air masses, which can be classified in continental arctic, when the air masses originate in northern of Russia and Novaya Zemlya, and in continental polar, when they come from Siberian plains. Focusing on Z500 anomaly (Fig. 6e), it is easy recognize a synoptic configuration that strongly departs from the classical schemes followed by atmospheric circulation on European area. The main features of this anomalous scenario lie in the presence of a high-pressure area extended from mid-Atlantic to Scandinavian Peninsula with a north-eastern to south-western axis. Moreover, there are two negative Z500 anomalies, one located over Greenland and Iceland and the other one across southern Italy. The latter is associated to a low-pressure area, located, on average, on Ionian Sea (Fig. 6f). According to this pattern, the central and eastern European territories experience stable but very cold weather, whereas the southern Italy is affected by cyclonic conditions that drives a north-eastern flow over the area of interest. Although the continental air masses are in general drier that maritime ones and so less prone to force clouds and precipitation formation, this synoptic set-up still supports snowfall events in the study area. In this respect, two important factors must be taken into account: the passage of cold continental air masses over the Adriatic Sea, which induces vertical transport of moisture and heat that enhance the instability, and the orographic forcing that come into play when the air masses interact with Partenio Mountains.

The ST4 (Mediterranean Low) depicts a large-scale flow conditioned by two relevant Z500 anomalies: one, of negative value, located across western and central Mediterranean basins, and the other one, of opposite sign, located over high latitudes (greater than ≈55°N) from northern Sea to Western Russia. This scenario, similarly to ST2, can be considered the result of a pronounced jet stream oscillation, bringing cold arctic or polar continental air masses towards southern Europe, and represent the final stage, i.e. cut-off low, of the Rossby wave evolution. The synoptic configuration sketched in Fig. 7a and Fig. 7b is synonymous of strong baroclinic conditions over central and southern regions of southern Italy and supports relevant snowfall events in the study area.

The ST5 (Arctic Trough) shows a mid-tropospheric scenario modulated by a wide trough, extended on European central meridians from Scandinavian Peninsula to central Mediterranean basins, and by a strong positive Z500 anomaly over mid-Atlantic (Fig. 7c). This pattern leads to cold arctic advection towards Italian peninsula, mainly of maritime origin. From the analysis of SLP pattern (Fig. 7d), three different pressure anomalies can be easily detected: a positive one over the Atlantic Ocean (which is compatible with a blocking high-pressure area) and two negatives, one over northern Europe and the other one across southern Italy and Balkan Regions. The meteorological set-up synthetized by ST5 is favourable to cyclonic conditions over the study area, which receives precipitation amounts mainly of convective nature (caused, for example, by the passage of a cold front, a comma or a cold occlusion).

https://doi.org/10.5194/tc-2021-363
Preprint. Discussion started: 23 December 2021

The first five ST discussed so far have some commonalities, mainly lying in the presence of a ridge over northern and central Atlantic (i.e. blocking high conditions), which results in very cold outbreak over most part of Europe. The ST6 (Polar maritime) depicts a very different pattern, which supports the incoming, over western and central Europe, of polar maritime air masses. By the inspection of Fig. 7e, four different Z500 anomalies can be detected: two of negative sign, located west of British Islands and over central Italy, and two of positive sign, situated over northern Europe and western Russia and south-western of Iberian Peninsula, respectively. The SLP anomalies (Fig. 7f) resemble the mid-tropospheric configuration and support cyclonic conditions over the study area, associated to convective precipitation events mainly triggered by sharp contrasts between cold air coming from north-western and milder Mediterranean air masses.

According to Table 2, the average frequency of occurrence (computed over the entire analysed period, 1884-2015) is quite homogeneous among various ST, i.e. there is not a dominant ST. In particular, ST4, ST6 and ST1 have, on average, the higher frequency of occurrence, 19.8, 19.3 and 17.7%, respectively. The remaining three patterns occur slightly less, but almost equally (12.1-16.3%). Moreover, we have averaged the amount of HNSd values recorded in the events triggered by each ST. The results, presented in Table 2, show that snowfall events are heavier when they are forced by a synoptic scenarios ascribable to ST4 (12.6 ± 10.8 cm), ST2 (12.0 ± 10.3 cm) and ST1 (11.8 ± 10.4 cm). The other three clusters (ST3, ST5 and ST6) are associated to average HNS_d values slightly lower mean (≈ 10 cm).

3.3 Variability in time of synoptic types

The information about the frequency of occurrence of the six ST have been extracted as follows. For each winter season of 1884-2015 period, we have identified the number of snowfall events associated to each cluster. The results are sketched in Fig. 8, where the temporal evolution of a determined ST frequency of occurrence is represented by the blue line and is expressed as number (#) of days per winter season. In order to filter out the high frequency variability, we have applied a lowess smoothing (red line), using a time window of 10 years. From a simple visual inspection of the six panels of Fig. 8, clearly emerges that none of the ST exhibit a defined linear trend, except for ST1, whose frequency of occurrence is affected by a negative tendency although not statistically significant.

To better isolate and discuss the behaviour in time of the signals presented in Fig. 8, we have evaluated the average frequency of occurrence of ST in each of the six sub-periods introduced in Section 3.1. Starting from ST1, its incidence on snowfall events in MVOBS gradually decrease from the first sub-period (1884/85-1906/07), where an average of 3.5 events has been detected, to the fourth temporal segment (1953/54-1974/75), when the mean frequency of occurrence was 2.8 days per winter season. Subsequently, there was a sharp decrease of the occurrence of this pattern, whose average frequency dropped to 1.9 days per winter season. In the last time segment (that ends up to 2014/15 season for this analysis), no relevant variations of average incidence of this ST has been detected. The ST2 has a quite irregular behaviour over the time. It is worth mentioning the lowering in average frequency of occurrence observed in the 1907/08-1929/30 period and, most importantly, the one

https://doi.org/10.5194/tc-2021-363
Preprint. Discussion started: 23 December 2021

detected in 1975/76-1997/98 period, when the average incidence of ST2 declined to 1.0 days per winter season. In this respect, there is a clear similarity with the previous cluster (ST1). In the last sub-period, there was a slight increase of the ST2 frequency, which, however, remains relatively low compared to the period before 1970s.

The ST3 also exhibit a very strong interannual variability. There is a common point with ST1 and ST2, lying in the decrease of frequency of occurrence observed in late 1970s and 1980s. However, from 1990s, there was a recovery of the incidence of this pattern, whose mean frequency remains quite stable until the end of the investigated period. The ST4 frequency of occurrence exhibit a negative trend in the first ≈ 40 years, a recovery in the period from 1930s to 1950s and then a decrease in 1953/54-1974/75 time segment. Subsequently, the time evolution of ST4 was modulated by a strong interannual variability; a slight greater incidence of this pattern on MVOBS snowfall events has been detected in the last fifteen years, when its frequency of occurrence was 2.8 events per year. The ST5 had a very high frequency of occurrence in the first years of XX century, and then its incidence rapidly dropped and remains almost stationary until the end of the analysed period. The ST6 has a similar behaviour: in the first 20 years, it exhibited a rising trend, maximizing its incidence in the 1910s, and then its frequency declined and remains quite stable over the time, except for a temporary decrease among 1980 and 2000s.

The key-findings of this analysis may be summarized as follows. In the period between 1970s and 1990s, when a strong reduction of snowfall events has been observed in MVOBS, there was a relevant decrease of ST2 and ST1 frequency of occurrence. The ST3 and ST6 also exhibited a lowering in their incidence in this period, although less prominent, whereas the ST4 and ST5 did not show any particular variations in their tendency. The recovery in snowfall amounts and number of events observed in MVOBS in the last sub-period may be related to the rising in frequency of ST3, ST4 and ST5, whereas the ST1 and ST2 incidence remains relatively low if compared to that observed prior 1970s.

Figure 9 provides further evidences about variability in time of the ST analysed in this study. It shows, for each of the six time intervals, the frequency of occurrence of ST relative to the total number of observed snow events. It is very interesting focusing on the integrated contribution of ST1 and ST2 (blue and red bars, respectively). In the first four time segments, it ranges from 28.4 (1907/08-1929/30 period) to 35.7% (1953/54-1974/75 period), then it strongly decreases to ≈ 24%. At the same time, it is worth of mention the increase in relative incidence of ST4 and ST5 (represented by magenta and green bars, respectively), which, in the last sub-period, account for the 43% of total snowfall events occurred in MVOBS.

At the light of these results, it is reasonable envisage that the alteration of MVOBS nivometric regime observed among 1970s and 1990s is strongly related to variations in large-scale atmospheric circulation. A comprehensive investigation about this aspect is offered in next section.

4 Relationship with teleconnection indexes

In this section, we investigate about connections between ST frequency of occurrence and five teleconnections patterns, introduced in paragraph 2.5, that have a large influence on Central Mediterranean atmospheric variability.

https://doi.org/10.5194/tc-2021-363
Preprint. Discussion started: 23 December 2021

Firstly, we have performed a simple linear correlation analysis between each ST and AO, NAO, EAWR, EMP and SCAND indices over the period 1950-2015. In computing the Pearson linear correlation coefficient (hereafter, *r*), we have considered only the winter seasons in which the value of a determined index belongs to its upper or lower quartile. This choice allowed better emphasizing the relationship between ST and positive and negative phases of teleconnection patterns (Cohen et al., 2013). The results are presented in Table 3, in terms of *r* and significance level (*p*); values in bold (grey) indicate correlations with 95% (90%) significance level. From a detailed inspection of Table 3, emerges that *r* values are generally lower than 0.5, except for ST2, which shows a very good agreement with NAO and AO indexes (r = -0.64 and -0.70, respectively); at the same time, it is important highlighting that all ST are correlated at the 95% significance level with at least one teleconnection index. In this respect, the only exception is the ST1, which has a low correlation degree with all indexes, although at 90% confidence level with NAO, AO and EMP. The ST3 is negatively correlated at 95% significance level with EMP and positively correlated at 90% with NAO and AO indices. The ST4 and ST5 are both positively correlated with EMP (r = 0.47 and 0.42, respectively); moreover, ST4 shows a good agreement with SCAND index, whereas ST5 is positively correlated with AO index (r = 0.40). The last cluster, ST6, exhibit a good linkage only with EAWR pattern (r = 0.48).

Figure 10 provides a more compelling evidence about the impact of positive (left panel) and negative (right panel) phase of teleconnection indices on the ST frequency of occurrence. The latter is expressed in terms of anomaly (number of days per winter season) with respect to 1981-2010 average. It is worth noting that a determined phase of a teleconnection index may have very different impacts on the ST regulating the snowfall regime in MVOBS. The positive phase of AO and NAO indexes determine a positive anomaly of ST3 frequency of occurrence and, conversely, a negative anomaly of ST1, ST2, ST4 and ST6. The opposite state of AO pattern (negative phase) is associated, as one would be expect, to an increase of ST1 and ST2. The negative phase of NAO index seems to exert an appreciable impact only on ST2, whose frequency of occurrence is higher in this circumstance, and on ST3 and ST5, which exhibit an incidence lower than normal. The positive phase of EMP index is clearly linked to a positive anomaly of ST1, ST3, ST4 and ST5 frequency of occurrence and, on the contrary, to a negative anomaly of ST6. The opposite is true for the negative phase. This result can be related to the synoptic scenario synthetized by the positive phase of EMP, characterized by a blocking ridge over north Atlantic that promotes polar or arctic cold air outbreaks across central Europe and Mediterranean regions. The SCAND pattern, in its positive phase, promotes a rising of ST3, ST4, and ST6 incidence, a weak increase of ST2 and ST5 and, at the same time, a decline of ST1 occurrence. The opposite state of this index has a remarkable link only with ST4, whose frequency of occurrence reduces to about 1.5 days per winter season. Regarding EAWR, both its positive and negative phase strongly affect ST2 and ST6, causing a lowering and an increase of the incidence of these patterns, respectively.

According to these findings, it may be helpful inspecting into the temporal variability of the teleconnections indices, to search connections with the time behaviour of the six ST identified in this study. In Figure 11 (left panel), we have condensed the wintertime series for 1950/51-2014/15 period of AO, EAWR, EMP, NAO and SCAND into a Hovmöller-like diagram. A detailed analysis of this figure reveals that the considered time interval may be subdivided into three sub-periods: 1950-mid-1970s, in which AO index is generally in its neutral or negative phase and a strong interannual variability prevail for the other

https://doi.org/10.5194/tc-2021-363
Preprint. Discussion started: 23 December 2021

patterns (and in particular for NAO index). Subsequently, from mid-1970s to the end of 1990s, when a strong reduction of snowfall amounts in MVOBS has been observed (see Fig. 11, right panel), both AO and NAO indices exhibited a positive trend. More specifically, the AO index was, on average, in its positive phase in mid-1970s, in early 1980s, between the end of 1980s and the beginning of 1990s and at the end of 1990s. In these periods, very strong positive anomalies of NAO index were also detected. Both patterns switched to the opposite state (i.e. negative) only at the end of 1970s and in middle of both 1980s and 1990s. From mid-1980s, positive phase of EAWR was also observed, especially in the first years of 1990s. The EMP and the SCAND resembles the behaviour taken in the precedent period, showing a strong interannual variability; it is important highlighting that a strong positive phase of these indices occurred in the mid-1970s (only for SCAND), in the early 1980s and in the first part of 1990s. In the last 15 years of the considered period, the AO index was generally weakly negative or neutral, except for the late 2000s, when a strong oscillation from positive to negative phase was observed. The NAO was generally neutral or positive, aside from the interval between the end of 2000s and the early 2010s, when a strong negative phase prevailed.

It is worth noting that from mid-1970s there is a near-systematic coupling between most relevant negative and positive AO and NAO events, in contrast with the previous time interval (i.e. 1950-mid 1970s), in which there was a prevalent decoupling. The evidences emerged from this analysis about NAO and AO indices were detailed discussed and related to the global warming phenomenon by Cohen and Barlow (2005). The latter concluded that the pattern and magnitude of the global warming trend in northern hemisphere over 1972-2004 period is largely independent of the AO and NAO. In other words, there is a strong divergence between trend in surface air temperature and tendency in AO and NAO indices.

The EAWR is neutral or positive until mid-2000s, and then neutral or negative phases prevailed. The EMP and the SCAND patterns do not show relevant tendencies: the first one was strongly positive in the mid-2000s and in early 2010s, whereas the second one was generally neutral and weakly negative, expect in the early 2010s, when the positive phase was dominant.

Based on the results of this analysis, it is very reasonable ascribe the negative snowfall amounts and number of events anomaly observed between 1970s and 1990s to the increase in NAO and AO indices values, which cause a reduction of the occurrence of some synoptic patterns, mainly ST1 and ST2, very favourable to the incoming, in Central Mediterranean area, of cold air masses of maritime (polar or arctic) origin. This achievement is in accordance with the findings of Merino et al. (2014), which attribute the decrease in the number of snow days observed in Castilla y León region (Spain) to the increase in the NAO index during winter months during the second half of the 20th century. The impact of NAO and AO anomalies was mitigated by the incidence of ST4 and ST5, which remains quite stable due to the occurrence of some periods characterized by positive values of EMP and SCAND indices. The increase in interannual variability of snowfall events detected in the last two decades, as well as the rise in the average amount, can be attributed to large-scale conditions more beneficial for cold outbreaks in central Mediterranean regions, as well represented by rising in frequency of negative AO patterns and by the occurrence of winter seasons modulated by positive EMP and negative EAWR.

https://doi.org/10.5194/tc-2021-363
Preprint. Discussion started: 23 December 2021

5 Conclusions

This work documents the snowfall variability observed from late 19th century to recent years in a remote Apenninic site (Montevergine) and prove its strong relationship with a wide range of large-scale atmospheric patterns that govern the winter variability in Central Mediterranean area.

Using a well-known cluster analysis technique (the k-means) and two meteorological fields (i.e. the 500-hPa geopotential heights and the sea level pressure) provided by the 20CRV3 reanalysis product, we have identified for the 1884/85-2014/15 period six different meteorological regimes (named "Arctic Maritime", "Central Europe Low", "Continental Air", "Mediterranean Low", "Arctic Trough" and "Polar Maritime"). The latter highlight that the linkage between Montevergine's snowfall variability and large-scale atmospheric circulation is very strong but also very complex. Two key-features that bring together the identified synoptic types are (i) the presence of a blocking high-pressure anomaly over north Atlantic and/or Scandinavian Peninsula and (ii) the genesis, in central Mediterranean area, of relevant baroclinic conditions, which constitute an essential ingredient for snow events. As testified by the cluster analysis, different meteorological scenarios, including outbreaks of cold air masses of both maritime and continental origin, can satisfy these conditions. In our opinion, this a first important result, which demonstrates the great relevance and representativeness of the long-term meteorological time series collected in Montevergine, which can be considered an ideal site for the study of climate variability in a "local-to-global framework", because its meteorological regime reflects a wide spectrum of large-scale atmospheric patterns.

The examination of the time variability of total winter snowfall amount and frequency of occurrence has revealed a very strong interannual variability as well as the absence of a relevant trend until the early 1970s. Subsequently, among 1970s and 1990s, there was a sharp decrease in snowfall amounts and in number of snowfall events (-45% and -17% compared to 1884-1975 period average, respectively). In the period from early 2000s to mid-2010s, the tendency in snowfall events number and amounts reverse and a more pronounced interannual variability has been newly observed.

With the aid of a supplementary analysis, we found a linkage between the identified synoptic types and five different teleconnection patterns that drive the European atmospheric variability, i.e. AO, EAWR, EMP, NAO and SCAND. Unfortunately, due to the limited availability of teleconnection indices data, this investigation is confined to the period 1950/51-2014/15. The "Arctic Maritime", "Central Europe Low" and "Polar Maritime" patterns are strongly connected, through a negative correlation, with AO, NAO and EAWR indices. The occurrence of the third synoptic type, "Continental Air", is partly related to AO, EMP, NAO and SCAND indices, whereas the "Mediterranean Low" pattern has connections with positive AO and NAO phases and with both positive and negative EMP and SCAND indices. The "Arctic trough" type has linkages with positive EMP phase and with negative AO, EAWR, EMP and NAO patterns.

The behaviour over time of some teleconnection indices, namely NAO, AO and EAWR, has leave a relevant footprint on Montevergine winter snowfall variability. From mid-1970s to the end of 1990s, these indices exhibited a trend towards positive phase, which determined a lowering of "Arctic Maritime" and "Central Europe Low" synoptic types occurrence. These two patterns play a relevant role in Montevergine nivometric regime, as testified by average daily snowfall amounts (11.8 and 12.0

https://doi.org/10.5194/tc-2021-363
Preprint. Discussion started: 23 December 2021

cm, respectively) associated with them. The increase in average of snowfall amounts observed in the last 15 years of the analyzed period can be explained by the reverse tendency of AO and EAWR indices, which results in a rise of "Arctic Trough", "Mediterranean low", "Continental Air" and "Central Europe Low" incidence.

To conclude, at the light of this study, the snowfall variability and trend observed in Montevergine in 1884-2015 period have been largely controlled by large-scale atmospheric variability. In the last past 40 years, when most of the global warming occurred, the investigated nivometric regime has been strongly modulated by AO and NAO patterns, which caused, mainly in the period between mid-1970s and 1990s, a strong reduction of synoptic-scale atmospheric patterns associated to maritime cold air advection.

Additional efforts, leave for future studies, should be devoted to the evaluation of the role exerted on the winter snowfall variability by the rising in temperature induced by global warming. In some previous works (e.g. Merino et al., 2014), this aspect is considered to have a strong impact on the snowfall trend and variability, although there is not a clear separation between its contribution and the one provided by large-scale atmospheric circulation patterns. The future perspectives also include the comparison between the evidences provided by Montevergine snowfall time series with other long-term nivometric data collected in Apennine environment or in the Alpine context. In this respect, we hope that our study can stimulate new efforts and actions to recover and valorise old snowfall records, especially in Italian territory, which has an inestimable asset of historical meteorological observations. Moreover, we aim to extend the analysis carried out in this work to spring and fall snowfall variability observed in Montevergine, to detect and discuss potential dissonances and similarities with the results obtained for winter season.

Code/Data Availability: The data that support the findings of this study are available from the corresponding author, upon reasonable request.

Competing interests. The authors declare that they have no conflict of interests.

Author contribution: Conceptualization, V.C.; methodology, V.C. and C.D.V.; formal analysis, V.C.; investigation, V.C.; resources, G.B.; writing—original draft preparation, V.C. and C.D.V.; writing—review and editing, G.B., C.D.V. and V.C.; supervision, G.B. All authors have read and agreed to the published version of the manuscript.

Acknowledgments. The authors of this work are very grateful to the Benedectine Community of Montevergine for affording the opportunity to analyse and digitise the old diaries and meteorological registers stored in Montevergine Abbey. In this respect, we address special thanks to Reverend Father Abbot Riccardo Guariglia and to Father Benedetto Komar.

https://doi.org/10.5194/tc-2021-363
Preprint. Discussion started: 23 December 2021

References

Ashcroft, L., Coll, J. R., Gilabert, A., Domonkos, P., Brunet, M., Aguilar, E., Castella, M., Sigro, J., Harris, I., Unden, P., and Jones, P.: A rescued dataset of sub-daily meteorological observations for Europe and the southern Mediterranean region, Earth System Science Data, 10, 1613–1635, https://doi.org/10.5194/essd-10-1613-2018, 2018.

Armstrong, R.L. and Brun E.: Snow and climate: physical processes, surface energy exchange and modelling. Cambridge, etc., Cambridge University Press, 256pp. ISBN-10: 0-521854-54-7, ISBN-13: 978-0-52185-454-7, Journal of Glaciology, 55(190), 384-384, https://doi.org/10.3189/002214309788608741, 2008.

Barnston, A. G. and Livezey, R. E., 1987: Classification, seasonality and persistence of low-frequency atmospheric circulation patterns. Mon. Wea. Rev. 115, 1083–1126, https://doi.org/10.1175/1520-0493(1987)115<1083:CSAPOL>2.0.CO;2, 1987.

Berghuijs, W.R., Woods, R.A. and Hrachowitz, M.: A precipitation shift from snow towards rain leads to a decrease in streamflow. Nature Climate Change, 4, 583-586, https://doi.org/10.1038/nclimate2246, 2014.

Braca, G., Bussettini, M., Lastoria, B., Mariani, S.: Anabasi – analisi stastistica di base delle serie storiche di dati idrologici – macro a supporto delle linee guida Ispra – manuale d'uso. Allegato in: Linee guida per l'analisi statistica di base delle serie storiche di dati idrologici. ISPRA, manuali e linee guida n.84/13, Roma, 2013.

Capozzi, V. and Budillon, G.: Detection of heat and cold waves in Montevergine time series (1884–2015), Adv. Geosci., 44, 35–51, https://doi.org/10.5194/adgeo-44-35-2017, 2017.

Capozzi, V., Cotroneo, Y., Castagno, P., De Vivo, C., Komar, A., Guariglia, R., and Budillon, G.: Sub-daily meteorological data collected at Montevergine Observatory (Southern Apennines), Italy from 1884-01-01 to 1963-12-31 (NCEI Accession 0205785), NOAA National Centers for Environmental Information, Dataset, https://doi.org/10.25921/cx3g-rj98, 2019.

Capozzi, V., Cotroneo, Y., Castagno, P., De Vivo, C., and Budillon, G.: Rescue and quality control of sub-daily meteorological data collected at Montevergine Observatory (Southern Apennines), 1884–1963, Earth Syst. Sci. Data, 12, 1467–1487, https://doi.org/10.5194/essd-12-1467-2020, 2020.

Changnon, S.A.: Catastrophic winter storms: An escalating problem, Climate Change, 84, 131–139, https://doi.org/10.1007/s10584-007-9289-5, 2007.

Cicogna, A., Cremonini, R., Debernardi, A., Faletto, M., Gaddo, M., Giovannini, L., Mercalli, L., Soubeyroux, J.-M., Sušnik, A., Trenti, A., Urbani, S., and Weilguni, V.: Observed snow depth trends in the European Alps: 1971 to 2019, The Cryosphere, 15, 1343–1382, https://doi.org/10.5194/tc-15-1343-2021, 2021.

Climate Prediction Center: https://www.cpc.ncep.noaa.gov/data/teledoc/telecontents.shtml, last access: 29 October 2021.

Cohen, J., and Barlow M., The NAO, the AO, and global warming: How closely related? J. Clim., 18, 4498– 4513, doi:10.1175/JCLI3530.1, 2005.

Cohen, L., S. Dean, and J. Renwick: Synoptic weather types for the Ross Sea region, Antarctica. J. Climate, 26, 636–649, https://doi.org/10.1175/JCLI-D-11-00690.1, 2013.

Cohen, J., Furtado, J., Barlow, M., Alexeev, V., and Cherry, J., "Arctic warming, increasing snow cover and widespread boreal winter cooling.", p. 1326, 2012.

Diodato, N.: Nota climatica ispirata alla serie storica delle precipitazioni osservate al Santuario di Montevergine, Rivista di Meteorologia Aeronautica, LII-N.34, 179–182, July–December, 1992.

Durre, I., Menne, M.J., Gleason, B.E., Houston, T.G. and Vose, R.S.: Comprehensive automated quality assurance of daily surface observations. Journal of Applied Meteorology and Climatology, 49, 1615–1633, https://doi.org/10.1175/2010JAMC2375.1, 2010.

Gadedjisso-Tossou, A., Adjegan, K.I. and Kablan, A.K.M.: Rainfall and Temperature Trend Analysis by Mann–Kendall Test and Significance for Rainfed Cereal Yields in Northern Togo. Sci, 3, 17. https://doi.org/10.3390/sci3010017, 2021.

Gao, P., Mu, X.M., Li, R. and Wang, W.: Trend and driving force analyses of streamflow and sediment discharge in Wuding River. J Sediment Res, 5, 22–28, 2009.

Hänsel Stephanie, Medeiros Deusdedit M., Matschullat Jörg, Petta Reinaldo A., de Mendonça Silva Isamara. Assessing Homogeneity and Climate Variability of Temperature and Precipitation Series in the Capitals of North-Eastern Brazil. Frontiers in Earth Science, 4, 29, DOI=10.3389/feart.2016.00029, 2016.

Hartnett, J.J., Collins, J.M., Baxter M.A., Chambers, D.P.: Spatiotemporal snowfall trends in Central New York. J Appl Meteorol Clim, 53, 2685–2697, DOI: 10.1175/jamc-d-14-0084.1 , 2014.

Hatzaki, M., Flocas, H.A., Giannakopoulos C. and Maheras P.: The impact of the eastern Mediterranean teleconnection pattern on the Mediterranean climate. Journal of Climate, 22, 977-992, https://doi.org/10.1175/2008JCLI2519.1, 2009.

Irannezhad, M., Ronkanen, A.K., Kiani, S. Chen, D. and Kløve, B.: Long-term variability and trends in annual snowfall/total precipitation ratio in Finland and the role of atmospheric circulation patterns, Cold Regions Science and Technology, 143, 2017, 23-31, https://doi.org/10.1016/j.coldregions.2017.08.008, 2017.

ISPRA, Fioravanti, G., Fraschetti, P., Perconti, W., Piervitali, E., Desiato, F.: Controlli di qualità delle serie di temperatura e precipitazione, 2016.

Kidson, J.W.: An automated procedure for the identification of synoptic types applied to the New Zealand region, Int. J. Climatol., 14, 711-721, https://doi.org/10.1002/joc.3370140702, 1994a.

Kidson, J.W.: The relation of New Zealand daily and monthly weather patterns to synoptic weather types. Int. J. Climatol., 14, 723-737, https://doi.org/10.1002/joc.3370140703, 1994b.

King C. and Turner J.: Antarctic Meteorology and Climatology, pp. 425. ISBN 0521465605. Cambridge, UK: Cambridge University Press, July 1997.

López-Moreno, J.I., Goyette, S., Vicente-Serrano, S.M. and Beniston M.: Effects of climate change on the intensity and frequency of heavy snowfall events in the Pyrenees. Climatic Change, 105, 489–508, https://doi.org/10.1007/s10584-010-9889-3, 2011.

MacQueen J.B.: Some Methods for classification and Analysis of Multivariate Observations, Proceedings of 5-th Berkeley Symposium on Mathematical Statistics and Probability, Berkeley, University of California Press, 1:281-297, 1967.

Marcolini, G., Bellin, A., Disse, M. and Chiogna, G.: Variability in snow depth time series in the Adige catchment, Journal of Hydrology: Regional Studies, 13, 2017, 240-254, https://doi.org/10.1016/j.ejrh.2017.08.007, 2017.

Matiu, M., Crespi, A., Bertoldi, G., Carmagnola, C. M., Marty, C., Morin, S., Schöner, W., Cat Berro, D., Chiogna, G., De Gregorio, L., Kotlarski, S., Majone, B., Resch, G., Terzago, S., Valt, M., Beozzo, W., Cianfarra, P., Gouttevin, I., Marcolini, G., Notarnicola, C., Petitta, M., Scherrer, S. C., Strasser, U., Winkler, M., Zebisch, M., Laternser, M. and

Schneebeli, M.: Long-term snow climate trends of the Swiss Alps (1931–99), Int. J. Climatol., 23, 733–750, https://doi.org/10.1002/joc.912, 2003.

Maugeri, M., Bellumé, M, Buffoni, L., and Chlistovsky, F.: Reconstruction of daily pressure maps over Italy during some extreme events of the 19th century, Il Nuovo Cimento, 21, 135–147, 1998.

Merino, A., Fernández, S., Hermida, L., López, L., Sánchez, J. L., García-Ortega, E. and Gascón, E.: Snowfall in the Northwest Iberian Peninsula: Synoptic Circulation Patterns and Their Influence on Snow Day Trends, The Scientific World Journal, 2014, 14, https://doi.org/10.1155/2014/480275, 2014.

Mu, X., Zhang, L., McVicar, T.R., Chille, B. and Gau, P.: Analysis of the impact of conservation measures on stream flow regime in catchments of the Loess Plateau, China. Hydrol Process, 21,2124–2134, DOI: 10.1002/hyp.6391, 2007.

Patakamuri, S.K., Muthiah, K. and Sridhar, V.: Long-Term Homogeneity, Trend, and Change-Point Analysis of Rainfall in the Arid District of Ananthapuramu, Andhra Pradesh State, India, Water, 12, 211. https://doi.org/10.3390/w12010211, 2020.

Pettitt, A. N., A non-parametric approach to the change point problem. Journal of the Royal Statistical Society Series C, Applied Statistics 28, 126-135, https://doi.org/10.2307/2346729, 1979.

Pons, M.R., San-Martín, D., Herrera, S., and Gutiérrez J.M.: Snow Trends in Northern Spain. Analysis and simulation with statistical downscaling methods, International Journal of Climatology, 30(12), 1795-1806, https://doi.org/10.1002/joc.2016, 2009.

Sheridan, S.C., and Lee C.C.: Synoptic climatology and the general circulation model. Prog. Phys. Geogr., 34, 101-109, DOI: 10.1177/0309133309357012, 2010.

Slivinski, L. C., Compo, G. P., Whitaker, J. S., Sardeshmukh, P. D., Giese, B. S., McColl, C., Allan, R., Yin, X., Vose, R., Titchner, H., Kennedy, J., Spencer, L.J., Ashcroft, L., Brönnimann, S., Brunet, M., Camuffo, D., Cornes, R., Cram, T.A., Crouthamel, R., Domínguez-Castro, F., Freeman, J. E., Gergis, J., Hawkins, E., Jones, P.D., Jourdain, S., Kaplan, A., Kubota, H., Blancq, F. L., Lee, T., Lorrey, A., Luterbacher, J., Maugeri, M., Mock, C. J., Moore, G. W. K., Przybylak, R., Pudmenzky, C., Reason, C., Slonosky, V. C., Smith, C. A., Tinz, B., Trewin, B., Valente, M. A., Wang, X. L., Wilkinson, C., Wood, K., and Wyszyński, P.: Towards a more reliable historical reanalysis: Improvements for version 3 of the Twentieth Century Reanalysis system, Q. J. Roy. Meteorol. Soc., 145, 2876–2908, https://doi.org/10.1002/qj.3598, 2019.

Smadi, M. M. and Zghoul, A.: A Sudden Change In Rainfall Characteristics In Amman, Jordan During The Mid 1950s. American Journal of Environmental Sciences, 2(3), 84-91, https://doi.org/10.3844/ajessp.2006.84.91, 2006.

Sneyers, R.: On the Statistical Analysis of Series of Observations. Technical Note No. 143, WMO No. 415, World Meteorological Organization, Geneva, 192, 1990.

Verstraeten, G., Poesen, J., Demarée, G., and Salles, C.: Long-term (105 years) variability in rain erosivity as derived from 10-min rainfall depth data for Ukkel (Brussels, Belgium): Implications for assessing soil erosion rates, J. Geophys. Res., 111, D22109, doi:10.1029/2006JD007169, 2006.

Wijngaard, J.B., Klein Tank, A.M.G. and Können, G.P.: Homogeneity of 20th century European daily temperature and precipitation series. Int. J. Climatol., 23, 679-692, https://doi.org/10.1002/joc.906, 2003.

Wilson, D., Hisdal, H. and Lawrence, D. Has streamflow changed in the Nordic countries? – Recent trends and comparisons to hydrological projections, Journal of Hydrology, 394 (3–4), 334-346, https://doi.org/10.1016/j.jhydrol.2010.09.010, 2010.

Winingaard, J.B., Kleink Tank, A.M.G. and Konnen, G.P. Homogeneity of 20th century European daily temperature and precipitation series. International Journal of Climatology, 23, 679– 692, DOI: 10.1002/joc.906, 2003.

World Meteorological Organization: Guide to Meteorological Instruments and Methods of Observation, 2008 Edition, WMO-no. 8 (Seventh edition), available at: https://www.wmo.int/pages/prog/www/IMOP/publications/CIMO-Guide/OLD-pages/CIMO_Guide-7th_Edition-2008.html (last access: 1 October 2019), 2008.

WMO, Guide to Climatological Practices (WMO-No. 100) Geneva: World Meteorological Organization, 2011.

Yeung, K.Y. and Ruzzo, W.L.: Principal Component Analysis for Clustering Gene Expression Data. Bioinformatics, 17, 763-774, http://dx.doi.org/10.1093/bioinformatics/17.9.763, 2001.

Zhang, S. and Lu, X.X.: Hydrological responses to precipitation variation and diverse human activities in a mountainous tributary of the lower Xijiang, China. Catena 77,130–142, https://doi.org/10.1016/j.catena.2008.09.001, 2009.

https://doi.org/10.5194/tc-2021-363
Preprint. Discussion started: 23 December 2021

The Cryosphere Discussions
Open Access
EGU

TABLES

Table 1. Average and standard deviation values (in cm) of total winter height of new snow (HNS) and number of snow days (NSD) observed in MVOBS for different sub-periods.

Sub-period	Total HNS	NSD
	Average and standard deviation (cm)	Average and standard deviation (number of days)
1884/85-1906/07	223.4 ±101.4	24.2 ±8.4
1907/08-1929/30	190.1 ±110.4	20.3 ±9.5
1930/31-1952/53	205.4 ±102.3	22.5 ±8.9
1953/54-1974/75	210.9 ±152.5	21.0 ±9.9
1975/76-1997/98	114.9 ±58.5	18.2 ±7.5
1998/99-2019/20	160.9 ±102.8	19.4 ±9.4

Table 2. For each of the six synoptic types, the average frequency of occurrence (in percentage) and the average and standard deviation (in cm) of daily height of new snow observed in MVOBS are shown. All parameters have been computed over the entire analysed period (1884-2015).

Synoptic Type	Frequency of occurrence (%)	Average and standard deviation of daily snowfall events (cm)
ST1 (Arctic Maritime)	17.7	11.8 (± 10.4)
ST2 (Central Europe Low)	12.1	12.0 (± 10.3)
ST3 (Continental Air)	14.8	9.8 (± 8.6)
ST4 (Mediterranean Low)	19.8	12.6 (± 10.8)
ST5 (Arctic Trough)	16.3	9.7 (± 7.9)
ST6 (Polar Maritime)	19.3	10.2 (± 9.0)

https://doi.org/10.5194/tc-2021-363
Preprint. Discussion started: 23 December 2021

765 **Table 3.** Linear correlation coefficient (*r*) between synoptic types frequency of occurrence and upper and lower quartiles of teleconnection indices over the period 1950-2015. Bold and grey values indicate correlations with 95% and 90% significance levels, respectively.

Synoptic type	NAO	AO	SCAND	EAWR	EMP
ST1	-0.30	-0.31	-0.29	-0.03	0.20
ST2	**-0.64**	**-0.70**	-0.04	**-0.46**	0.07
ST3	0.33	0.38	0.22	0.13	**0.37**
ST4	-0.14	-0.17	**0.40**	-0.01	**0.47**
ST5	0.29	0.40	0.07	0.14	**0.42**
ST6	-0.34	-0.29	0.18	**-0.48**	-0.15

770

775

780

785

790

https://doi.org/10.5194/tc-2021-363
Preprint. Discussion started: 23 December 2021

FIGURES

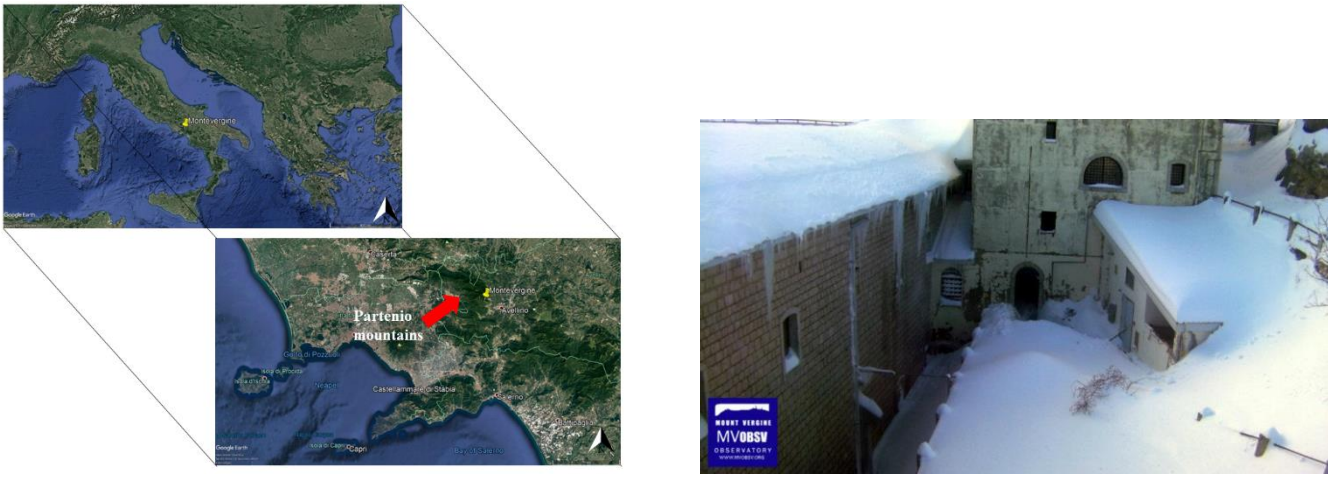

Figure 1: On left panels, the Italian and Balkan peninsulas (in the upper) and the Campania region (in the bottom) are shown. The location of Montevergine observatory is highlighted via a yellow pin, whereas the red arrow indicates the Partenio Mountains. Images credits: © Google Earth, Data Sio, NOAA, U.S. Navy, NGA, GEBCO. The right panel shows a picture (taken on 15 Feb. 2012) of the "*Giardinetto dell'Ave Maria*", a cloister of the Montevergine Abbey where snow measurements have been performed over the time. Image credits: non-profit organization "MVOBSV – Mount Vergine Observatory".

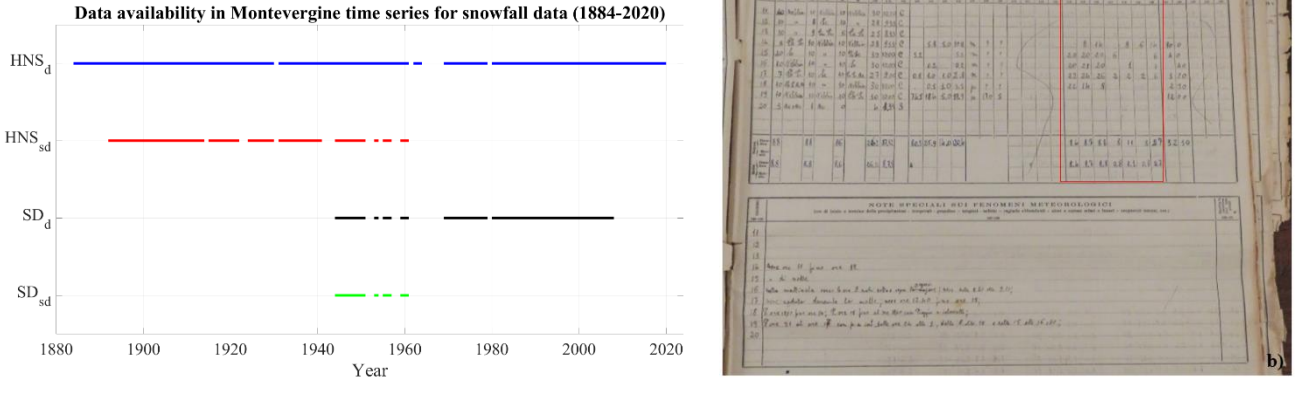

Figure 2: The left panel shows the data availability of snowfall measurements in Montevergine dataset in the period ranging from 1884 to 2020. HNS$_d$ (blue line) stands for daily height of new snow, HNS$_{sd}$ (red line) for sub-daily height of new snow, SD$_d$ (black line) for daily snow depth and SD$_{sd}$ (green line) for sub-daily snow depth parameter. Near-continuous observations are available only for the daily height of new snow (HNSd) parameter. The right panel presents an example of the original data source (related to the second 10-day period (i.e. from day 11 to 20) of January 1946). Each row accounts for the observations of a specific day, and each column is devoted to the records of a determined parameter at a specific hour of the day. The columns including snowfall measurements are bordered with red lines.

https://doi.org/10.5194/tc-2021-363
Preprint. Discussion started: 23 December 2021

The Cryosphere Discussions
Open Access
EGU

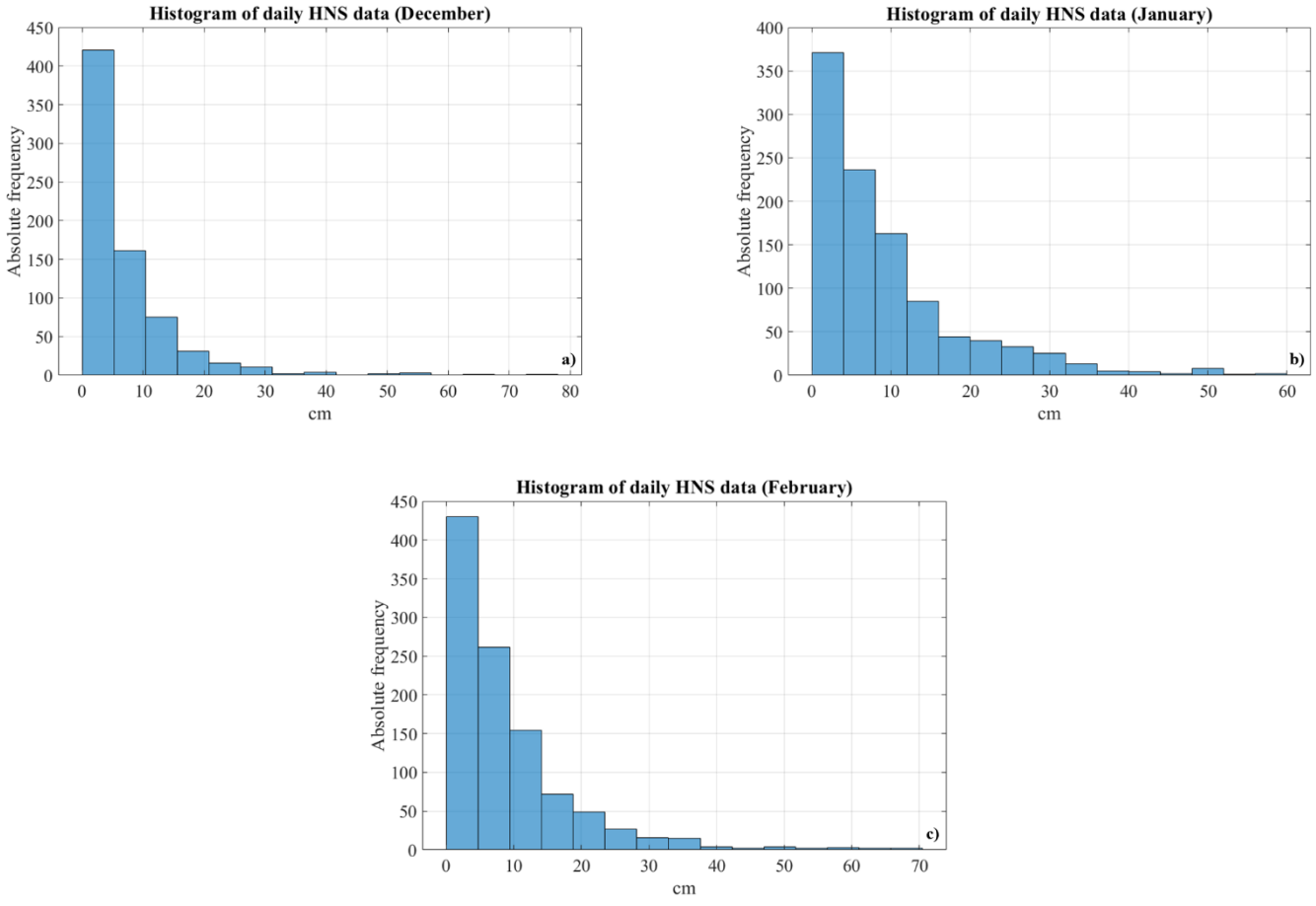

Figure 3: Histograms of daily height of snow (HNSd) observed in MVOBS in December (a), January (b) and February (c). The y-axis is the absolute frequency (expressed as number of days), whereas the x-axis is the HNSd amount at the bin centre (in cm). Data collected between 1884 and 2020 have been taken into account.

https://doi.org/10.5194/tc-2021-363
Preprint. Discussion started: 23 December 2021

The Cryosphere Discussions
Open Access
EGU

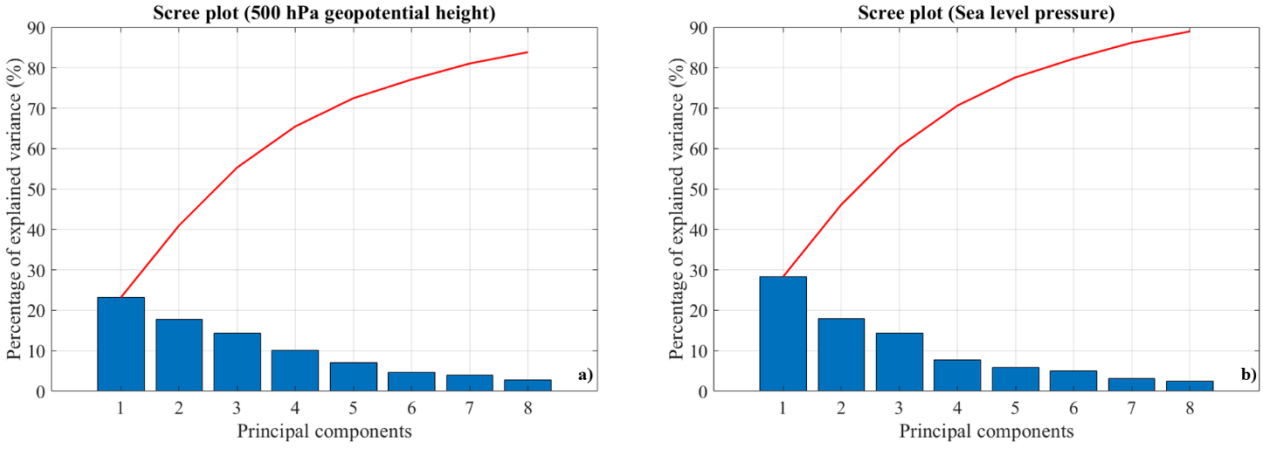

Figure 4: Scree plot of variance (blue bars) and cumulative variance (red line) for the first eight principal component of the two parameters involved in cluster analysis, the 500-hPa geopotential height (a) and the sea level pressure (b). The data have been retrieved from 20CRV3 dataset, considering only winter snow days occurred in MVOBS between 1884 and 2015.

820

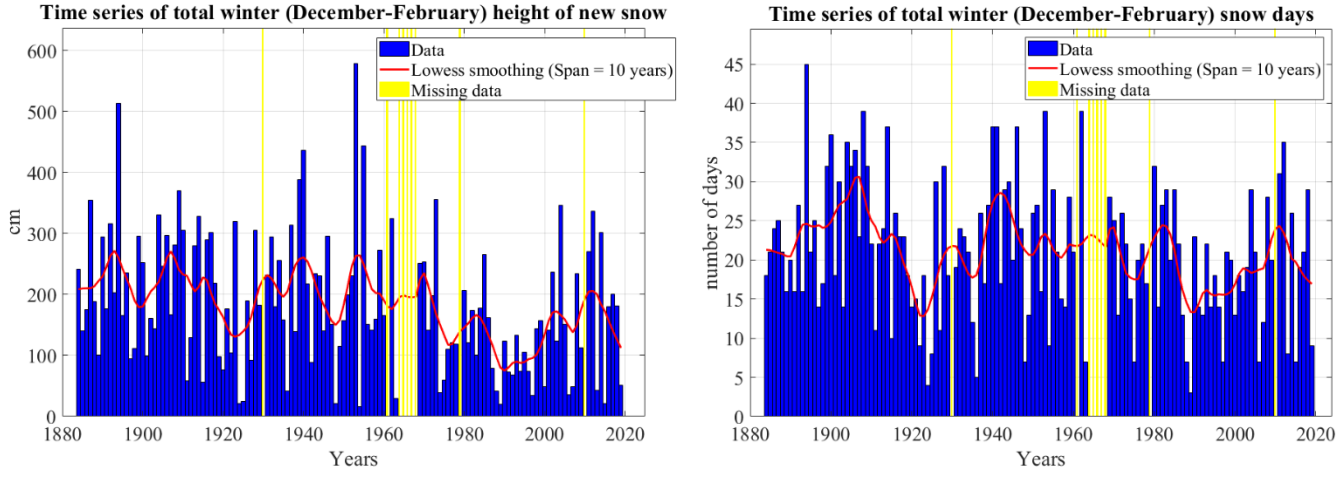

Figure 5: Winter (December to February) time series of total height of new snow (left panel) and total number of snow days (right panel). In both panels, the missing data are highlighted as yellow bars. The red line shows the 10-year locally weighted scatter plot smooth (lowess).

825

https://doi.org/10.5194/tc-2021-363
Preprint. Discussion started: 23 December 2021

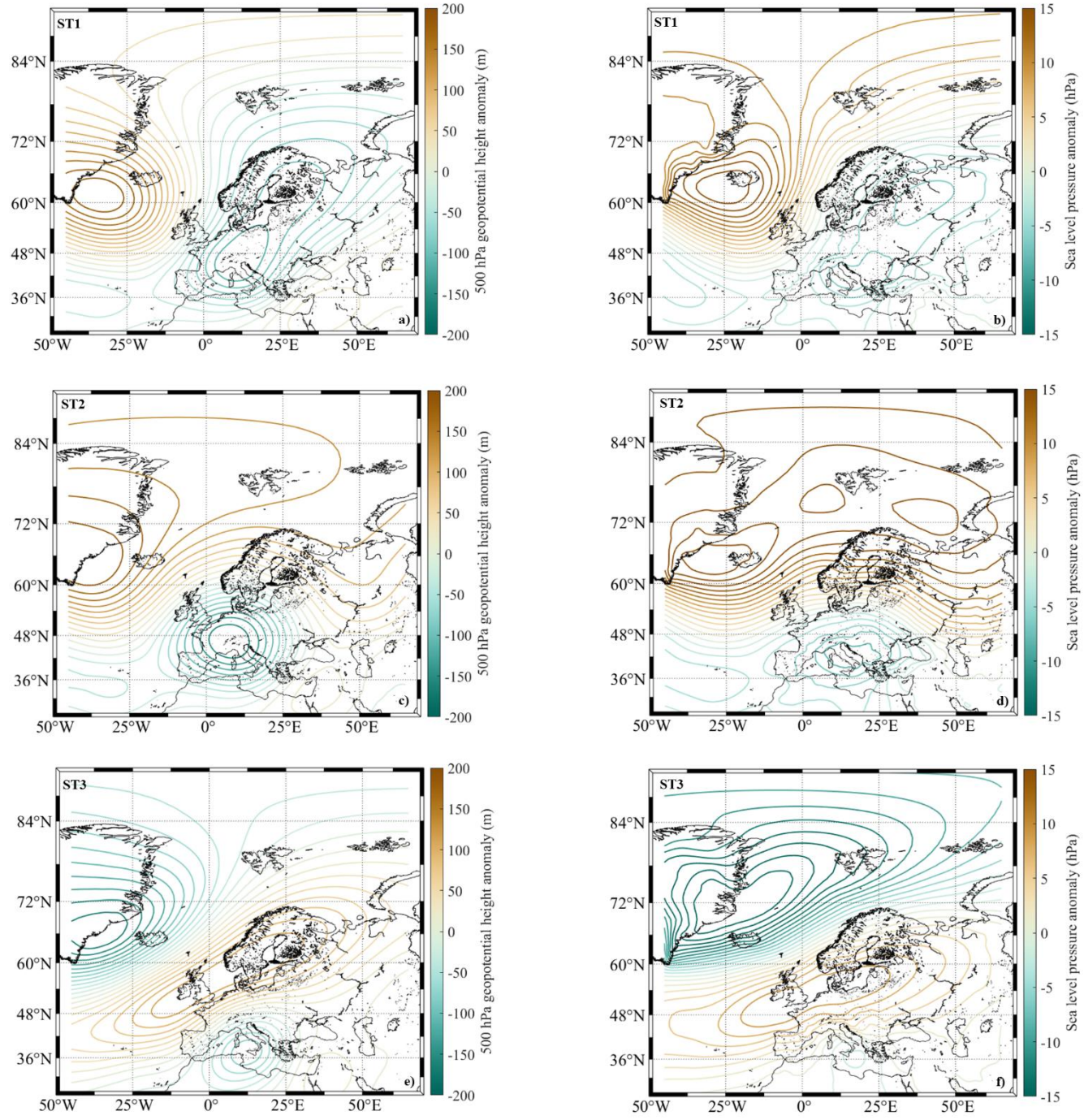

Figure 6: Synoptic types (ST) controlling the snowfall events and variability in MVOBS. More specifically, this figure sketches the ST1 ("Arctic Maritime"), the ST2 ("Central Europe Low") and the ST3 ("Continental Air"). The left panels (a, c and e) show, for ST1, ST2 and ST3, respectively, the 500-hPa geopotential height anomaly (in m) with a contour interval of 20 m; the right panels (b, d and f) present the sea level pressure anomaly (in hPa) with a contour interval of 1.5 hPa. The ST have been obtained from 20CRV3 reanalysis product (1884-2015 period), considering an area embracing the entire European territory (25-90°N, -45-65°E).

https://doi.org/10.5194/tc-2021-363
Preprint. Discussion started: 23 December 2021

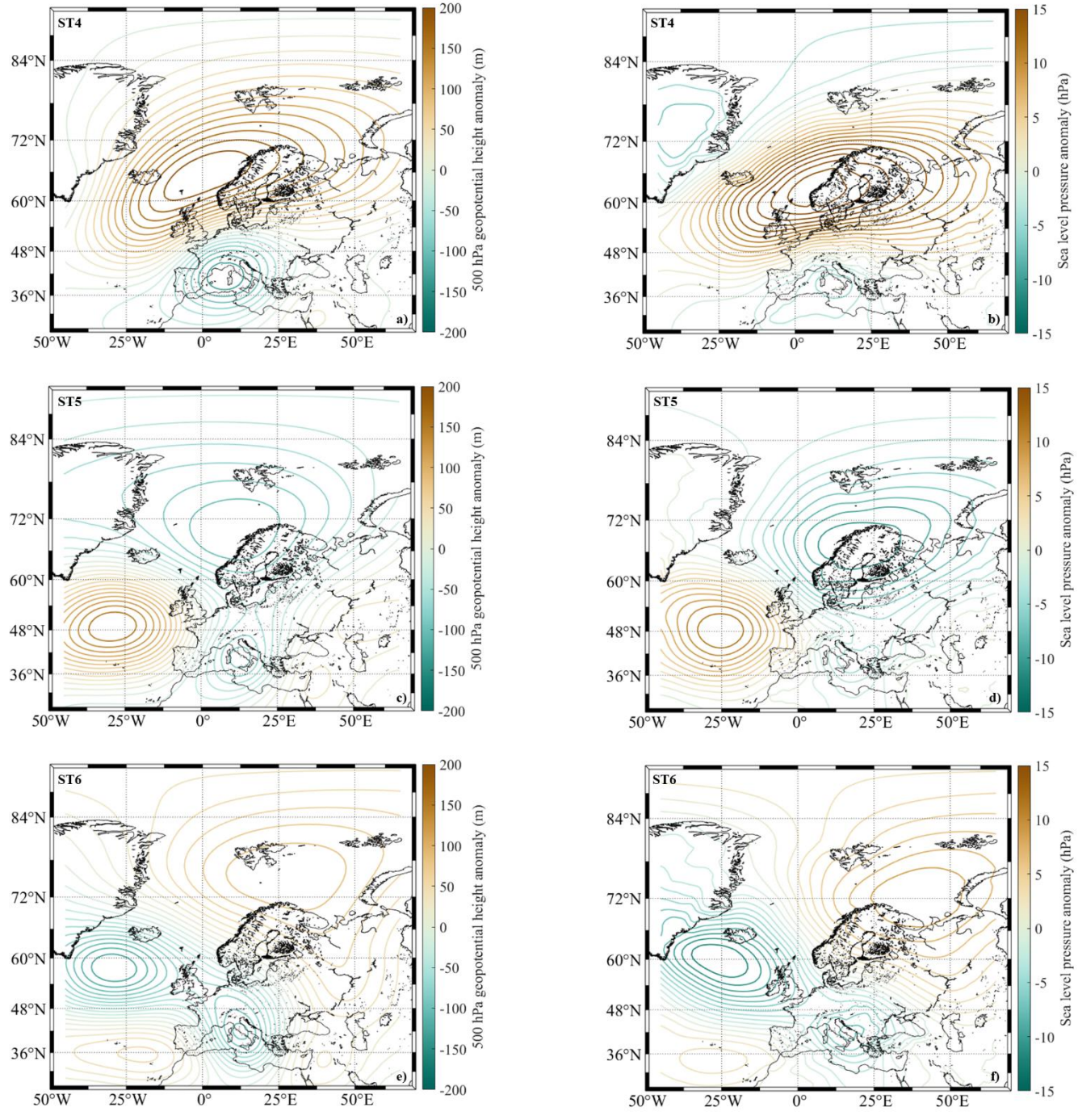

Figure 7: Synoptic types (ST) controlling the snowfall events and variability in MVOBS. More specifically, this figure sketches the ST4 ("Mediterranean Low"), the ST5 ("Arctic Trough") and the ST6 ("Arctic Maritime"). The left panels (a, c and e) show for ST4, ST5 and ST6, respectively, the 500-hPa geopotential height anomaly (in m) with a contour interval of 20 m; the right panels (b, d and f) present the sea level pressure anomaly (in hPa) with a contour interval of 1.5 hPa. The ST have been obtained from 20CRV3 reanalysis product (1884-2015 period), considering an area embracing the entire European territory (25-90°N, -45-65°E).

https://doi.org/10.5194/tc-2021-363
Preprint. Discussion started: 23 December 2021

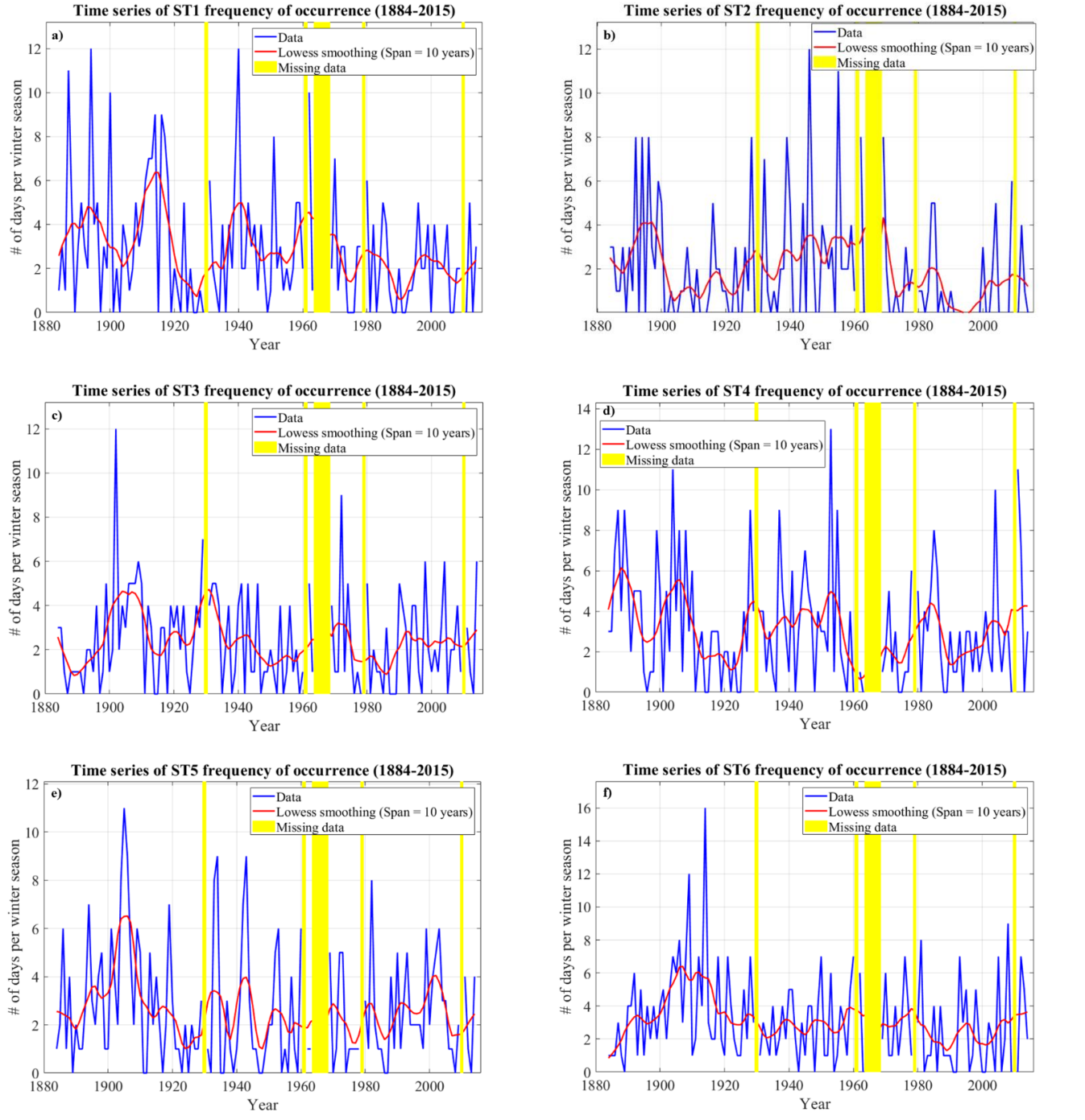

Figure 8: Time series of the frequency of occurrence, expressed in terms of number of days per winter season, of the six synoptic types (ST) emerged from the cluster analysis, i.e. ST1 (a), ST2 (b), ST3 (c), ST4 (d), ST5 (e) and ST6 (f). In all panels, the missing data are highlighted as yellow bars, whereas the red line shows the 10-year locally weighted scatter plot smooth (lowess). The period from 1884 to 2015 has been considered.

https://doi.org/10.5194/tc-2021-363
Preprint. Discussion started: 23 December 2021

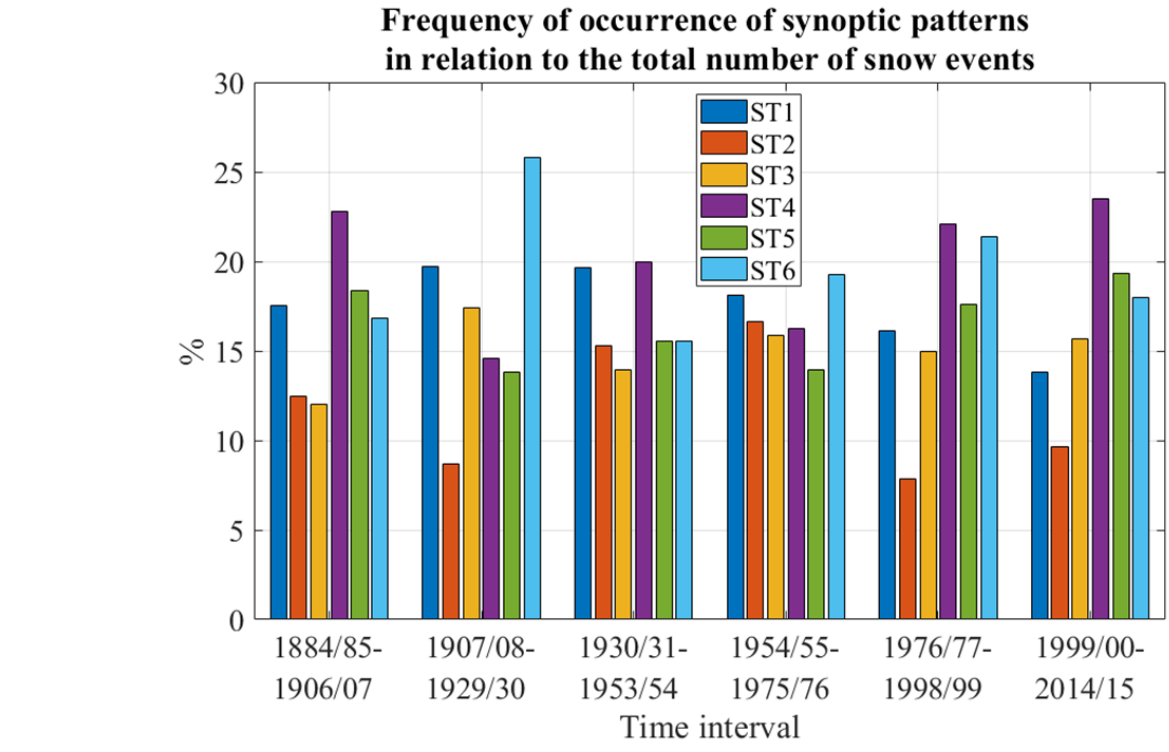

Figure 9: Each group of bar represent the frequency of occurrence of ST (expressed as percentage) in relation to the total number of snowfall events observed in a determined time interval. The six synoptic types, i.e. ST1, ST2, ST3, ST4, ST5 and ST6, are marked as blue, red, orange, magenta, green and cyan bars, respectively.

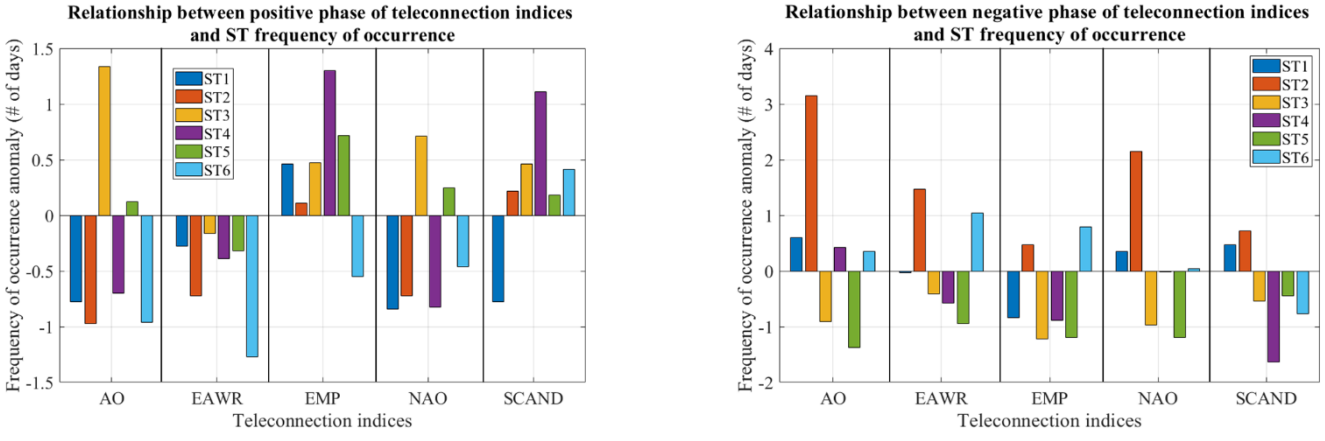

Figure 10: For the positive (left panel) and negative (right panel) phase of the teleconnection indices involved in this study, i.e. the Arctic Oscillation (AO), the Eastern Atlantic Western Russia (EAWR), the Eastern Mediterranean Pattern (EMP), the North Atlantic Oscillation (NAO) and the Scandinavia pattern (SCAND), the frequency of occurrence anomaly of the synoptic types is

https://doi.org/10.5194/tc-2021-363
Preprint. Discussion started: 23 December 2021

860 **shown. The anomalies are expressed in number of days and they have been computed with respect to 1981-2010 period. The six synoptic types, i.e. ST1, ST2, ST3, ST4, ST5 and ST6, are marked as blue, red, orange, magenta, green and cyan bars, respectively.**

865

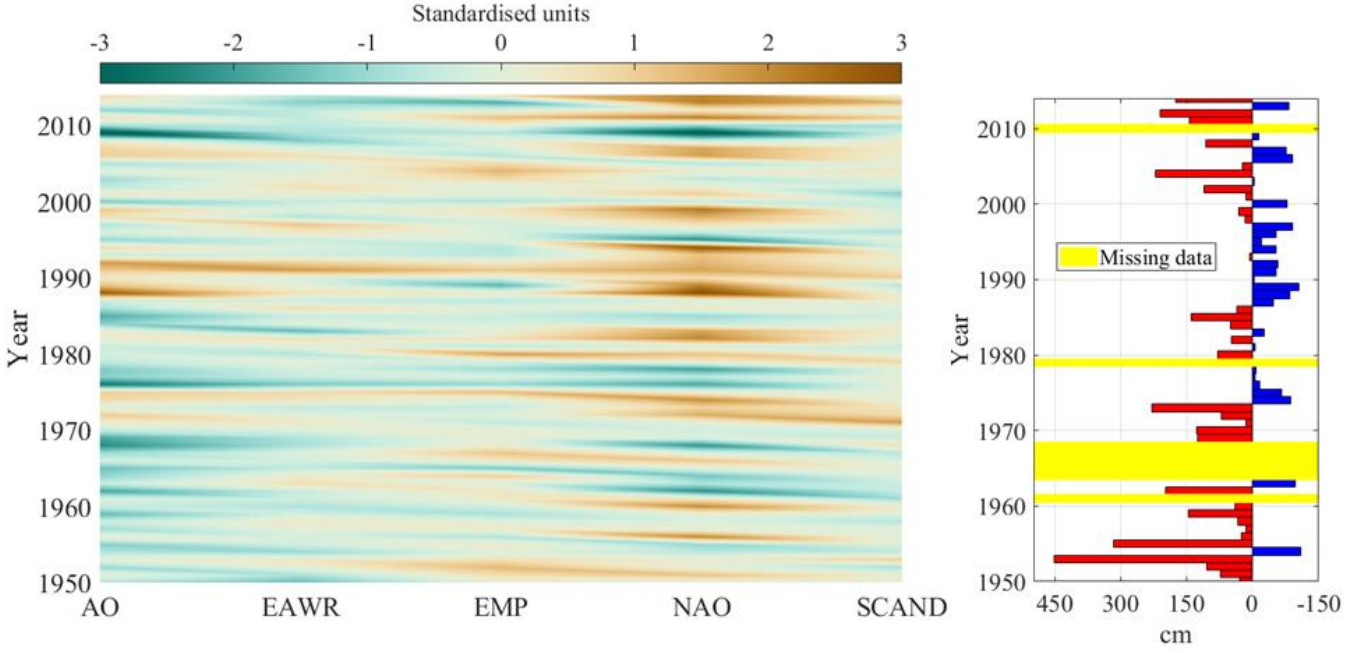

Figure 11: The left panel presents the behaviour in time of the teleconnection indices adopted in this study, in the form of a Hovmöller-like diagram. More specifically, in the x-axis the winter value of Arctic Oscillation (AO), Eastern Atlantic Western Russia (EAWR), Eastern Mediterranean Pattern (EMP), North Atlantic Oscillation (NAO) and Scandinavia pattern (SCAND) is show from
870 **left to right. The indices values are color-coded according to the horizontal bar and are expressed as standardized units. The right panel shows the winter (December to February) time series of total height of new snow, expressed as anomalies (in cm) with respect to 1981-2010 period. Red bars highlight winters with positive anomaly (in cm), blue bars winters with negative anomaly. The missing data are marked as yellow bars. For both panels, the period 1950/51-2014/15 is considered.**